Technical Report Documentation Page

1. Report No. FHWA/TX-07/0-4307-1	2. Government Accession No.	3. Recipient's Catalog No.
4. Title and Subtitle Design Guidelines For Steel Trapezoidal Box Girder Systems		5. Report Date April 2007 6. Performing Organization Code
7. Author(s) Todd Helwig, Joseph Yura, Reagan Herman, Eric Williamson, Dawei Li		8. Performing Organization Report No. 0-4307-1
9. Performing Organization Name and Address Center for Transportation Research The University of Texas at Austin 3208 Red River, Suite 200 Austin, TX 78705-2650		10. Work Unit No. (TRAIS) 11. Contract or Grant No. 0-4307
12. Sponsoring Agency Name and Address Texas Department of Transportation Research and Technology Implementation Office P.O. Box 5080 Austin, TX 78763-5080		13. Type of Report and Period Covered Technical Report (09/01/01 – 08/31/04) 14. Sponsoring Agency Code

15. Supplementary Notes
Project performed in cooperation with the Texas Department of Transportation and the Federal Highway Administration.

16. Abstract

The frequency of use of steel box girders has increased in the state of Texas and throughout the United States over the past 10 years. Some of the advantages of the structural shape that have led to the increased utilization include improved aesthetic, maintenance, and structural benefits. Geometric continuity is achieved since the trapezoidal shape of the steel girders match the prestressed concrete U-beams that are frequently used in Texas. The smooth shapes of the girders also provide a sleek appearance as shown in Figure 1.1. In addition, since the girders are closed they tend to remain dry and there are fewer places for debris and other corrosion causing agents to collect. However, the primary advantage of box girders is the large torsional stiffness that makes the girders ideal for use in curved interchanges for which the bridge geometry can lead to large torques. The torsional stiffness of a box section is generally in the range of 100 to more than 1000 times larger than that of a comparable I-shaped section. While the large torsional stiffness has led to increased use in curved girder applications, there also have been a number of applications in which the girders have been used in straight bridge applications to match adjacent prestressed concrete U-beams. In these cases, straight steel box girders are used in regions where the clear span requirements preclude the use of the concrete U-beams.

17. Key Words Steel, Box Girders, Trapezoidal, Torsional	18. Distribution Statement No restrictions. This document is available to the public through the National Technical Information Service, Springfield, Virginia 22161; www.ntis.gov.

19. Security Classif. (of report) Unclassified	20. Security Classif. (of this page) Unclassified	21. No. of pages 84	22. Price

Form DOT F 1700.7 (8-72) Reproduction of completed page authorized

Design Guidelines For Steel Trapezoidal Box Girder Systems

Todd Helwig
Joseph Yura
Reagan Herman
Eric Williamson
Dawei Li

CTR Technical Report:	0-4307-1
Report Date:	April 2007
Project:	0-4307
Project Title:	Steel Trapezoidal Girders: State of the Art
Sponsoring Agency:	Texas Department of Transportation
Performing Agency:	Center for Transportation Research at The University of Texas at Austin

Project performed in cooperation with the Texas Department of Transportation and the Federal Highway Administration.

Center for Transportation Research
The University of Texas at Austin
3208 Red River
Austin, TX 78705

www.utexas.edu/research/ctr

Disclaimers

Author's Disclaimer: The contents of this report reflect the views of the authors, who are responsible for the facts and the accuracy of the data presented herein. The contents do not necessarily reflect the official view or policies of the Federal Highway Administration or the Texas Department of Transportation (TxDOT). This report does not constitute a standard, specification, or regulation.

Patent Disclaimer: There was no invention or discovery conceived or first actually reduced to practice in the course of or under this contract, including any art, method, process, machine manufacture, design or composition of matter, or any new useful improvement thereof, or any variety of plant, which is or may be patentable under the patent laws of the United States of America or any foreign country.

Engineering Disclaimer

NOT INTENDED FOR CONSTRUCTION, BIDDING, OR PERMIT PURPOSES.

J. A. Yura, P.E, Texas No. 29859
T.A. Helwig, P.E., Texas No. 92480
E. B. Williamson, P.E., Texas No. 94410

Research Supervisors

Acknowledgments

The authors express appreciation to Tom Fan, Project Director (Houston District); Richard Wilkison, Program Coordinator (Bridge Division); John Holt, Project Monitoring Committee (Bridge Division); John Vogel, Project Monitoring Committee (Houston District).

Products

This report is Product 1, Design Guide for Trapezoidal Girders.

Table of Contents

Table of Figures

Chapter 1

Introduction and Overview

1.1 Introduction

The frequency of use of steel box girders has increased in the state of Texas and throughout the United States over the past 10 years. Some of the advantages of the structural shape that have led to the increased utilization include improved aesthetic, maintenance, and structural benefits. Geometric continuity is achieved since the trapezoidal shape of the steel girders match the prestressed concrete U-beams that are frequently used in Texas. The smooth shapes of the girders also provide a sleek appearance as shown in Figure 1.1. In addition, since the girders are closed they tend to remain dry and there are fewer places for debris and other corrosion causing agents to collect. However, the primary advantage of box girders is the large torsional stiffness that makes the girders ideal for use in curved interchanges for which the bridge geometry can lead to large torques. The torsional stiffness of a box section is generally in the range of 100 to more than 1000 times larger than that of a comparable I-shaped section. While the large torsional stiffness has led to increased use in curved girder applications, there also have been a number of applications in which the girders have been used in straight bridge applications to match adjacent prestressed concrete U-beams. In these cases, straight steel box girders are used in regions where the clear span requirements preclude the use of the concrete U-beams.

Figure 1.1 Trapezoidal Box Girder Bridge

Although there are significant structural advantages to box girders in many bridge applications, the basic requirements and design methodologies for a number of key structural elements are not well established for bridge designers. While there were a number of research investigations conducted on steel box girders during the 1960's and 1970's, there was a long period of inactivity during the 1980's and early 1990's that led to relatively antiquated design methodologies. In many situations, design methodologies did not exist for several key structural elements. As a result, "typical sizes" have been employed for some of the structural elements and the details that have been employed have covered a wide spectrum. The lack of established design methodologies and consistent details complicates the design, fabrication, and construction of these bridges. The Texas Department of Transportation (TxDOT) has funded a number of studies since 1995 to improve the understanding of the behavior of curved steel box girders. These studies have focused on the behavior of the overall superstructure as well as the bracing systems that are used for the girders.

The purpose of this design guide is to provide a summary of the current understanding of the behavior of box girder systems as well as presenting preferred practices and design recommendations for the different structural elements that comprise single-celled trapezoidal box girder systems. The recommendations in this publication are intended to supplement the codes and standards presented in the AASHTO Bridge Design Specifications (2007) as well as the TxDOT Bridge Design Manual (2001). Another good source of information for design reference is the Preferred Practices for Steel Bridge Design, Fabrication, and Erection (2005).

The remainder of this chapter provides an overview of some of the basic terminology and structural concepts applicable to trapezoidal box girder bridges. Following this introductory section, an overview of the geometrical shape of trapezoidal boxes is provided as well as a discussion of some of the primary components that comprise the box girder systems. A basic discussion of torsional theory is then provided. Finally an outline of the remaining chapters of the design guide is presented.

1.2 Trapezoidal Box Girder Geometry

Conventional single-cell steel box girders are designed to act compositely with the concrete deck in the finished bridge. Since the concrete deck closes the box section, the as-fabricated steel girders are typically comprised of a bottom flange, two webs, and two top flanges as shown in Figure 1.2. The sloping webs of the girders lead to a trapezoidal shape, which is where the origin of the commonly-used name trapezoidal box girders is derived. While the sloping webs produce a sleek appearance to the girders that enhance the overall aesthetics, there are also practical structural reasons for the inclined webs such as reducing the bottom flange width. In addition to reducing the amount of material required for the bottom flange, the smaller width helps with local plate buckling in regions around supports where the bottom flange is in compression.

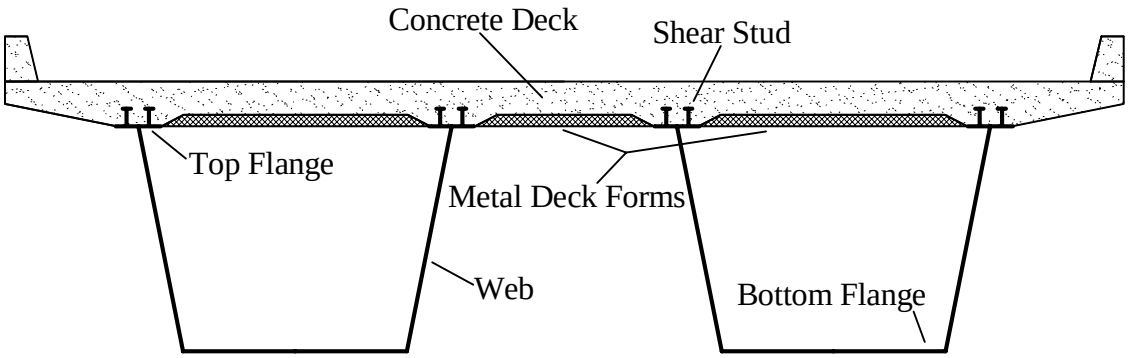

Figure 1.2 Typical Cross Section of Trapezoidal Box Girder System

The size of the top flange in the region of positive bending (compression in the top of the girder) is often relatively small as depicted in the figure since the composite bridge deck will provide a large structural element that dramatically increases the bending and torsional stiffness. In the negative moment region, the combined area of the top flanges often approach the corresponding bottom flange area since bending causes tension in the top of the girder for which concrete is relatively ineffective. Although the small top flanges reduce the amount of steel required in the girder, the discontinuity in these flanges results in an open section that is relatively flexible in torsion. Therefore, there are a number of bracing systems that are required to improve the performance of the girders. Most of these bracing systems are required primarily during construction of the concrete bridge deck, however much of the bracing is left on the finished bridge. Both internal and external bracing systems are used on the boxes. Some of the typical internal braces are depicted in Figure 1.3.

Figure 1.3a shows a typical internal K-frame. The individual components that make up the trussed brace are referred to as a strut and a diagonal. The primary purpose of the internal K-frames is to control distortion of the box girder. Although different types of truss systems are possible for the internal cross-frames, a K-frame such as the one depicted in the figure is most often used since the opening in the middle facilitates access in walking down the middle of the box during construction or routine maintenance inspections.

A lateral truss such as the one depicted in Figure 1.3b is required at or near the top flange of girders to control the torsional flexibility during girder erection and construction. The plan view of the bracing system shows that like the internal K-frames, the individual components of the truss are referred to as struts and diagonals. The strut of the top flange truss also serves as the strut of the internal K-frame. During construction, a steel box with the top flange lateral truss is often referred to as a quasi-closed box since the primary purpose of the top truss is to simulate the stiffness of a closed box system. Even in straight girder systems with little or no torsional load, the top flange truss is required for girder stability during construction. From a torsional perspective, the lateral truss may be viewed as a fictitious plate with a purpose to effectively close the open

section. As will be discussed in Chapter 3, this leads to one of the design approaches named the "equivalent plate method" that may be used to size the top flange truss.

Figure 1.4 shows a picture of a recently erected twin box girder. External K-frames are often positioned at intermediate points along the bridge length. The primary purpose of these braces is to help control the relative twist of adjacent box girders, thereby achieving a uniform slab thickness. Due to fatigue concerns, these intermediate braces are usually removed from the completed bridge.

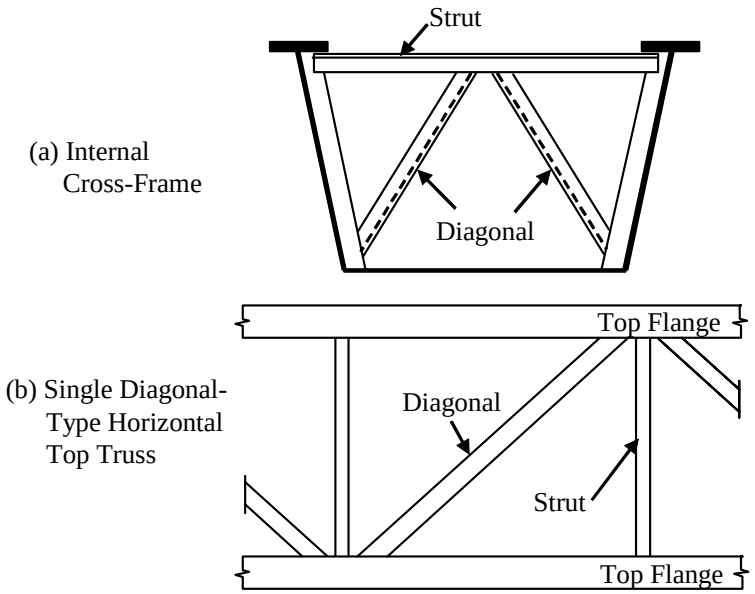

Figure 1.3 Typical internal box girder bracing systems

Figure 1.4 External box girder bracing

An external K-frame or a solid plate diaphragm is required at the supports of the bridge to resist twist of the girder. If a cross-frame is provided, a K-frame system is usually employed. Stiffening plates are typically required at the top and bottom of solid plate diaphragms resulting in an I-shaped section.

The ends of the individual box girders are closed with a solid plate diaphragm. Solid plate diaphragms are also used within each girder above interior supports of continuous girders. Access ports are required at these intermediate diaphragm locations to allow inspection personnel to move from one span to the next during routine maintenance inspections. Since these diaphragms are typically positioned directly over the support bearings, vertical stiffeners are typically required to handle the girder reactions. Although elastomeric bearing pads have been successfully employed in some steel box girder applications, pot bearings have been utilized the most often. The main purpose of these bearings is to allow the girders to expand and contract to accommodate daily and annual thermal changes that the bridge undergoes as well as accommodating construction and live load rotations.

When establishing the girder geometry for bridges, the preferable layout is for the supporting pier lines to be normal to the longitudinal axis of the girders in straight bridges and to be oriented along a radial line to the girder curvature in curved bridges. However, in some cases, the bridge geometry or geographical aspects necessitate that the girder supports must be skewed from the radial lines. The design requirements for the bracing can be affected by the orientation of the supporting piers. A brief discussion of torsional theory is provided in the following section.

1.3 Torsional Theory

Torsional moments in thin-walled sections such as box girders are resisted by the shear stresses on the components that make up the girder cross-section. Torsion in thin-walled members is usually categorized as either Saint-Venant torsion or warping torsion. Saint-Venant torsion is the result of pure shear deformations in the plane of the plates that comprise the thin-walled member, while warping torsion is associated with the bending deformations in the plane of the individual plates. Although both Saint-Venant and warping torsion are developed in box girder sections, Saint Venant torsion often dominates the stiffness of the closed cross-section. The longitudinal normal stresses due to warping torsion are usually negligible (Kollbrunner and Basler 1969).

The large Saint-Venant stiffness of a box girder provides a torsional stiffness that may be 100~1000 times that of a comparable I-section. The torsional stiffness of a thin-walled box section is a function of the shear modulus of the material, G, and the torsional constant, K_T, which is related to the geometric profile of the cross-section. The following expression relates the resistance of the cross-section to the torsional stiffness (Kollbrunner and Basler 1969):

$$M_T = GK_T \frac{d\phi}{dx} , \qquad (1.1)$$

where M_T is the torque on the cross-section of the member, G is the shear modulus, ϕ is the rotation of the cross-section, and x denotes the longitudinal axis of the member. The torsional constant for thin-walled single cell box girders is given by

$$K_T = \frac{4A_0^{\,2}}{\sum_i b_i / t_i} \ , \qquad (1.2)$$

where A_0 is the enclosed area of the cross-section of the box girder, b_i and t_i in the summation are the respective width and thickness of the *i*th plate in the box.

The shear stress due to Saint-Venant torsion can be solved using Prandtl's membrane analogy (Kollbrunner and Basler 1969). For example, for girders with a single cell cross-section, a uniform shear flow, q, develops along the perimeter of the box and can be determined using Bredt's equation as follows:

$$q = \tau t = \frac{M_T}{2A_0} \ , \qquad (1.3)$$

in which t is the thickness o f the plate, and τ is the shear stress, which is essentially uniform through the thickness of the plates. The distribution of torsional shear stress is demonstrated in Figure 1.5.

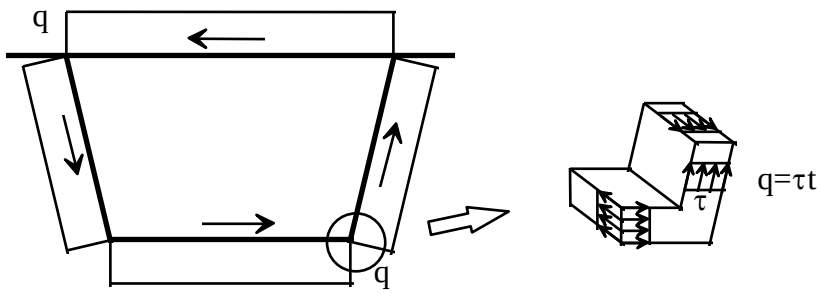

Figure 1.5 Shear Flow in Box Girder Due to Saint-Venant Torsion

The torsional warping stresses in the box girder are usually negligible. However, significant warping stresses due to the cross-sectional distortion of box girders may develop. The shear flow distribution given by Equation 1.3 is based upon the assumption that the cross-section of the box girder maintains the original shape. Torsional loads on box girders usually result from either eccentric loads or the bridge geometry. Although the torsional moment can be applied so as not to distort the cross-section, under general torsional loads, the cross-sections of box girders will distort from the original profile. Box girder distortion results in additional longitudinal warping stresses as well as out-of-plane bending stresses in the individual plates of the box girder sections (Dabrowski 1968). The distortional stresses in the box girder are a function of the box girder

geometry and the magnitude of the distortional load. A more detailed discussion of cross-sectional distortion is presented in Chapter 4.

1.4 Design Guide Overview

The research presented in this design guide was sponsored by the Texas Department of Transportation. The Guide provides a summary of several studies on the basic behavior of trapezoidal box girders systems. The studies have included laboratory and field investigations as well as parametric finite element analyses. An analytical tool named UTrAp was also developed in the TxDOT sponsored research to aid designers in predicting stresses induced in the bracing members and girder cross-sections of trapezoidal box girder systems. The Guide has been divided into five chapters.

Chapter 2 focuses on analysis methods for box girder systems. The chapter provides a discussion of the benefits and shortcomings of commonly used grid models that are used to analyze curved girder systems. In addition, an overview of the UTrAp program is provided.

Chapter 3 provides a discussion of the behavior and design requirements of the top flange lateral truss that is provided to achieve a quasi-closed box section. The general behavior of the top flange truss as a function of box girder torsion and vertical bending due to flexure is discussed. Simplified hand solutions to capture the truss forces induced by both torsion and box girder bending are presented as well as recommended details.

Chapter 4 provides an overview of the basic requirements for the internal K-frames that are provided to control box girder distortion. In addition to presenting equations to predict the forces induced by box girder distortion, recommended details are outlined.

Chapter 5 discusses the basic design and detailing requirements for external bracing systems such as K-frames and solid plate diaphragms. Equations are given to estimate the spacing requirements between the external K-frames and expressions are also given to estimate the design forces in the members. The design requirements for solid plate diaphragms at supports are also discussed. Expressions for the plate diaphragms that consider the strength and stiffness requirements are presented.

Chapter 2

Analysis Methods

2.1 Introduction

Although bridge systems are often complex three-dimensional structures, past and present design practices often simplify the modeling of bridges to expedite the structural analysis. For example, a straight multi-girder bridge will often experience significant three-dimensional effects from design trucks that can be placed in a multitude of positions both longitudinally and transversely on the bridge. While it would be possible to model the multi-girder system relatively accurately, most designers analyze the behavior of an individual girder and employ live load distribution factors to account for the interaction of girders in resisting the truck loads. In most straight girder applications, the simplified analysis is warranted, and the live load distribution factors have been calibrated to produce good estimates of the actual girder moments and shears.

Although simplified analysis techniques are possible with curved girder applications, the system behavior can be quite complex due to the three-dimensional nature of the curved profile. Dramatic improvements in the speed and data storage of personal computers throughout the 1990s have made sophisticated three-dimensional modeling of bridge systems a viable option for bridge designers. While a three-dimensional model of the girder system is preferred, most commercially available software for bridges employ a grid analysis in which the complex nature of the girders and other structural members are modeled as line elements. In these analyses, the engineer must compute the section properties of the girder and specifically input these properties for the different cross-sections of the girders and bracing members. The accuracy of a grid analysis may not be sufficient in certain cases, and an engineer should have a good understanding of the basic assumptions upon which the analysis is based.

There are many pros and cons of both grid analysis techniques and three-dimensional modeling that an engineer must consider when selecting analytical software. In many applications, a grid analysis can produce good estimates of the distribution of moments, shears, and torques on the girders. However, the grid analysis will not provide any information of local distortions and also does not reflect the behavior of many of the bracing systems that are commonly employed. Subsequent chapters will provide expressions that designers can use to predict forces in the bracing members as well as lateral bending stresses in the girder flanges. When these expressions are combined with grid analyses solutions, the girder systems can be proportioned to support the design loads in an efficient manner.

The design expressions that will be presented in later chapters can help an engineer in understanding the origin of the many components that contribute to the

resultant forces in the bracing members; however, many of these effects can be accurately predicted using a three-dimensional model of the girders. The program UTrAp is a three-dimensional finite element analysis (FEA) program that has been configured to permit a designer to quickly model a box girder system with a Graphical User Interface (GUI) that is relatively simple to use.

The remaining three sub-sections of this chapter focus on methods of analysis for box girder systems. Three different methods of torsional analysis are discussed ranging from the very simple to relatively robust methods. The first technique to be discussed is the *M/R* method, which utilizes analytical results from straight girder systems and approximates the effects of horizontal curvature. The next method to be discussed is grid modeling, which although the geometrical curvature is built into the model, significant geometrical approximations are employed to simplify the torsional analysis. The final section focuses on three-dimensional modeling, which is the most complex analysis method, but it is also the most geometrically accurate procedure. The section on three-dimensional modeling highlights the abilities of the program UTrAp.

2.2 M/R Method

A relatively simple analysis method for curved box girder bridges is the *M/R* method developed by Tung and Fountain (1970). Although the method is based upon the assumption that bridges have a small to medium curvature, the method is effective for a wide range of curved highway bridges. For example, bridges with as much as 40° subtended angle between two torsionally-fixed supports can be analyzed using the *M/R* method (Tung and Fountain 1970). Because the radius is assumed to be relatively large when applying this method, it is assumed that the effect of curvature on the bending behavior of a curved girder is negligible. The bending moment of the girder can be determined by neglecting the curvature and using traditional beam theory for straight girders. Therefore, bending moments are determined in the first step of the *M/R* method by assuming the girder is straight with the spans equal to the developed lengths of the curves.

Torsional moments in curved girders can be induced by the curvature of girder alignment even without direct torsional load on the girders. This effect can be represented by an equivalent distributed torsional load, *M/R*, for which the method is named. The basic mechanics of the procedure are illustrated in Figures 2.1 through 2.3. Figure 2.1 depicts a horizontally curved box girder of radius *R*, and a uniformly distributed load of *w*. The distributed load will cause bending moments distributed along the length of the girder. The forces in the flanges from bending can be approximated by dividing the moment, *M*, by the depth of beam, *h*, as shown in Figure 2.2. The *M/h* force acting on the curved segment is shown in Figure 2.2a. The curvature in the segment leads to a lateral component of $(M/h)d\theta$ acting on the flange. If this lateral force is divided by the length of the segment, *ds*, a distributed lateral load equal to *M/(Rh)* results. The effect of the curvature can thus be approximated by a straight model in which the flange segment is subjected to the longitudinal force of *M/h* and an external distributed load of *M/(Rh)* in

the lateral direction as depicted in Figure 2.2b. The bottom flange is also subjected to the same amount of the lateral load but in the opposite direction. As a result, these two horizontal components form a distributed torsional load equal to *M/R* acting on the girder as shown in Figure 2.3. Therefore, the torsional moments due to the curvature of the girder are approximately equal to the torsional moments in a straight beam due to the distributed torsional load of *M/R*.

In addition, there may exist other direct torsional loads such as those due to vertical loads eccentric to the shear center of the girder. The torsional analysis due to M/R as well as other torsional loads can be approximated by neglecting the curvature of the girder. Therefore, the M/R method does not require a curved beam model for both the bending and torsional analysis. If twist is prevented at all supports, the torsional analysis can be performed by considering only one span at a time because torsional warping is usually very small in box girders, and, therefore the torsional deformation in one span does not significantly affect adjacent spans.

The assumption used in the M/R method is also the basis of the V-Load method for curved I-girder bridges. Instead of the shear flow developed on cross-sections of box girders, the equivalent torque M/R is resisted by the warping-type non-uniform bending of different girders in the I-girder system (Richardson 1963).

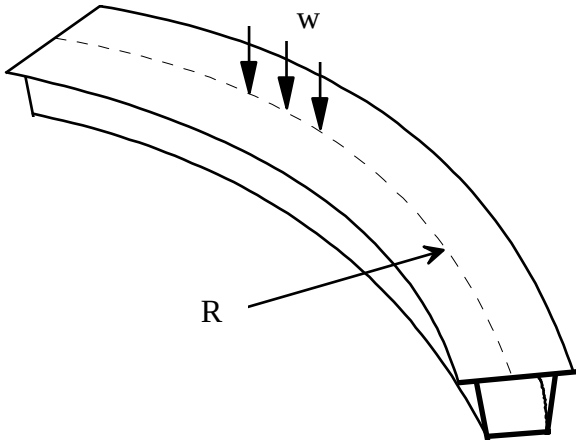

Figure 2.1 Curved Box Girder Under Vertical Loads

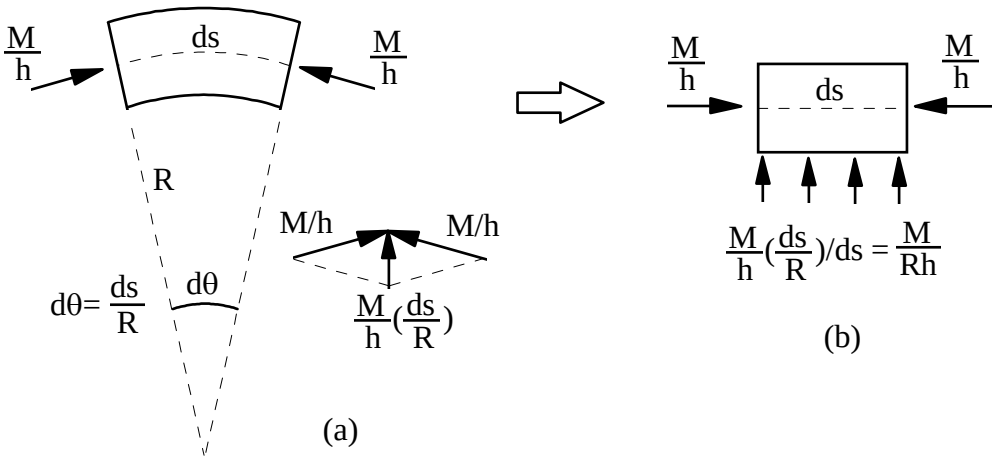

Figure 2.2 Approximation of the Effect of Curvature on Box Girder Flanges

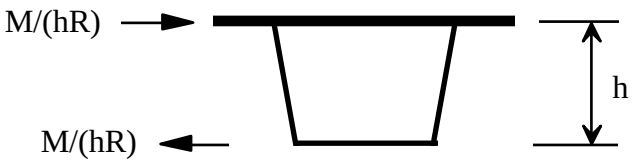

Figure 2.3 Equivalent Torsional Loads on Curved Box Girder

2.3 Grid Analyses

Most commercially available software specifically applicable to bridges is based upon a grid analysis. There are a number of attractive features to these software packages including ease of use and automated checks of the AASHTO Specifications. Dealing with an analysis on a large bridge system can be daunting to many engineers, and the simplified nature of the grid analysis method can greatly expedite the learning curve on the software. From this perspective, an engineer can create an analytical model of a horizontally curved bridge in a relatively short period of time. In addition, because the simplified models often have a relatively small number of degrees of freedom, the user is not significantly hindered by the speed of the computer on which the analysis is conducted. Another attractive aspect of these software packages is that the programs have been developed to perform live load checks with design trucks or lane loads.

However, while checking the behavior of the bridge in-service is obviously an important and necessary design step that an engineer must evaluate, many of the

commercially available software packages are relatively ill-prepared to check bridge behavior during erection and construction. From a design perspective, the most critical stage for the bracing systems is during construction. The engineer must be able to accurately model the quasi-closed box girder and consider the casting sequence of the concrete to evaluate the critical load stages that cause the largest brace forces and girder stresses. A grid analysis cannot provide brace forces in the internal K-frames or top flange truss, nor can the engineer directly capture local distortions that might occur in complicated regions of the structure.

While the engineer can calculate properties of the closed box section and use approximations such as the Equivalent Plate Method (discussed in Chapter 3) to simulate the top flange truss, modeling many of the bracing members such as the external cross-frames can be quite difficult. For example, consider the twin box system shown in Figure 2.4. The spacing between the center of the two boxes is 240 inches. In a grid analysis, the external K-frame would often be modeled as a single line element spanning the full 240 inches between the center of the two girders. In reality, the actual bracing consists of two internal K-frames and an external K-frame. Approximating the stiffness of the internal and external bracing systems can be complicated, and the results reported from a grid analysis are often going to be unreliable for such bracing configurations. As is discussed in Chapter 5, a more reliable approach to designing the intermediate external K-frames is to consider these braces to aide in satisfying constructability requirements of for the concrete bridge deck. In designating the external K-frames in a constructability role, these braces would not be included in the structural analysis. As a result, the girder and end diaphragms would be sized to have sufficient strength to resist the full construction loading. Typical sizes can then be used on the intermediate external K-frames so as to control the relative twist of two adjacent box girders. While this approach does not ensure that the external K-frames will be free from problems during construction, a safe system will typically result because the diaphragms at the support and the girder cross-sections are sized to support the entire torques. In addition, the resulting girder twists from analysis without the external diaphragms will not be too large due to the significant torsional stiffness of the quasi-closed section. Expressions for the spacing and force requirements for the external K-braces are provided in Chapter 5.

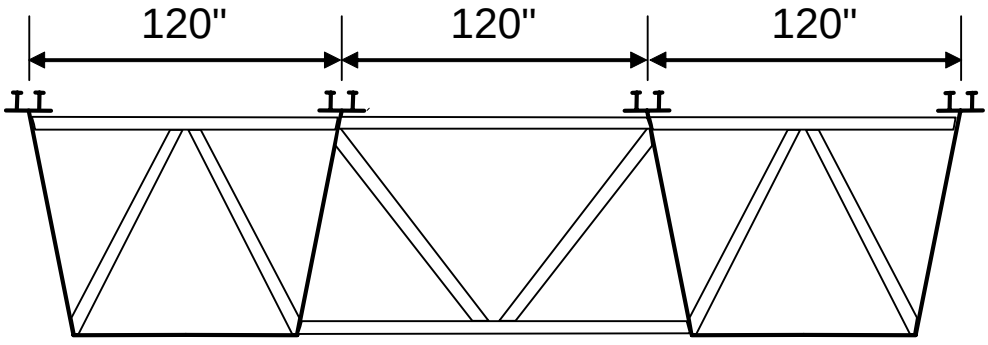

Figure 2.4 Cross Section of Twin Girder Bridge at Intermediate Location

While a similar problem as discussed with modeling intermediate cross-frames exists with the plate diaphragms at the supports, the line element model as used in a grid analysis is perhaps more reasonable in this situation because the interior diaphragm plates and exterior solid plate diaphragms form a continuous element. Problems can still arise with grid models of bridges with a skewed support at one end of a span. At a skewed support, the diaphragm has two moment components: one oriented transverse to the girder and another oriented in the longitudinal direction of the girder. With a skewed support at one end only, the in-plane rotation of the girder causes forces in the plate diaphragm that affect the distribution of torque along the girder length. As a result, the torsion diagram is generally shifted up or down depending on whether the exterior or interior girder is considered. Provided an accurate value for the torsional constant is input for the quasi-closed section, the grid analysis will provide reasonable estimates of the torque. However, the accuracy of the grid model is very sensitive to the torsional constant that is specified as was shown by Helwig, Herman, and Li (2004).

2.4 Three Dimensional FEA

An alternative to utilizing the simplified grid modeling techniques is to explicitly model the plate elements that comprise the girders as well as the bracing members using three-dimensional FEA. While grid modeling techniques do result in efficient models by limiting the number of degrees of freedom in the analysis, significant increases in the speed and data storage capabilities of personal computers over the past decade have made three-dimensional FEA modeling a viable option for design engineers. The limiting factor in choosing between a grid model and a three dimensional FEA model is not usually related to hardware, but it is often related to the availability of suitable analysis programs. As mentioned in the last subsection, most commercially available software for bridges is based upon a grid analysis methodology. While there are several three-dimensional FEA programs that can be used to model straight and curved bridges, very few of these packages are specifically targeted at bridges. Instead, these software programs are general purpose analysis packages that can be used to model a variety of structures. The flexibility of these programs allows the user to create detailed models of very complex structures; however, a great deal of time is often necessary for users to become proficient at using the many features offered by such software packages.

With the finite element method, complex structures are divided into a large number of elements for which the behavior of each element is well defined. The response of the system being modeled is then computed by simply summing the effects of all the elements that comprise the model. Because the behavior of each element is known, the resulting system of equations, while perhaps very large, is readily solved. The finite element approach offers the advantages of being able to model the spatial configuration of a bridge and the ability to determine the stress and strain distribution at any location in a cross-section. Because the cross-section is modeled by a large number of finite elements, its actual shape is used for the analyses. As such, no assumptions are needed for defining section properties such as the torsional constant. Furthermore,

bracing members can be modeled directly using beam or truss elements. Consequently, the analyst need not resort to modeling the section as pseudo-closed using the Equivalent Plate Method.

In order to take advantage of the inherent strengths associated with finite element modeling, an easy-to-use software package (UTrAp) with a graphical user interface (GUI) was developed for the analysis of curved steel box girders under construction loads. The package consists of an analysis module and a GUI, and it was developed for use on personal computers. Unlike commercially available general-purpose FEA software, UTrAp allows engineers to quickly and easily define bridge geometry and a corresponding finite element mesh. After the bridge response is computed, analysis results are provided through the GUI to allow engineers to visualize the behavior of the analyzed bridge system. Users of the software do not need to have extensive experience with FEA to obtain accurate predictions of response. In the paragraphs below, an overview of the software is provided, and the capabilities and limitations are discussed.

The analysis module consists of a three-dimensional finite element program with pre- and post-processing capabilities. Input for the analysis module is provided by a text file that is created through use of the GUI. The module itself is capable of generating a finite element mesh, element connectivity data, and material properties based on the geometrical properties supplied through the GUI. The program also generates nodal loading based on the values given in the input file. After the pre-processing is completed, the program assembles the global stiffness matrix and solves the equilibrium equations to determine the displacements corresponding to a given analysis case. As a last step, the module post-processes the displacements in order to compute cross-sectional forces, stresses and brace member forces.

The program is capable of generating output useful to designers based on the displacements computed from the analyses. Output obtained from post-processing is written to text files that can be read through use of the GUI. The program outputs vertical deflection of the girder centerline as well as the cross-sectional rotation along the length of the bridge. In addition, the program calculates axial forces for all top lateral, internal, and external braces. Cross-sectional stresses and forces are calculated at two-foot intervals along the bridge length. For each cross-section, shear and normal stresses are printed out at 26 and 52 locations for single and dual girder systems, respectively. These stress components are given in the local directions (i.e., normal and perpendicular to the cross-section). In addition to stresses, cross-sectional shear, moment, and torsion are calculated at two-foot intervals along the length of the bridge.

The Graphical User Interface was designed to provide an environment in which a user can easily enter the required input data. In addition, the GUI has the capability of displaying both the numerical and graphical output of the analysis results. Figure 2.5 shows the main form of the interface, and viewing from top to bottom, it displays the

plate thickness properties, pour sequence, and the plan view of the bridge. Figure 2.6 shows the interface in which users enter dimensions of the bridge being analyzed.

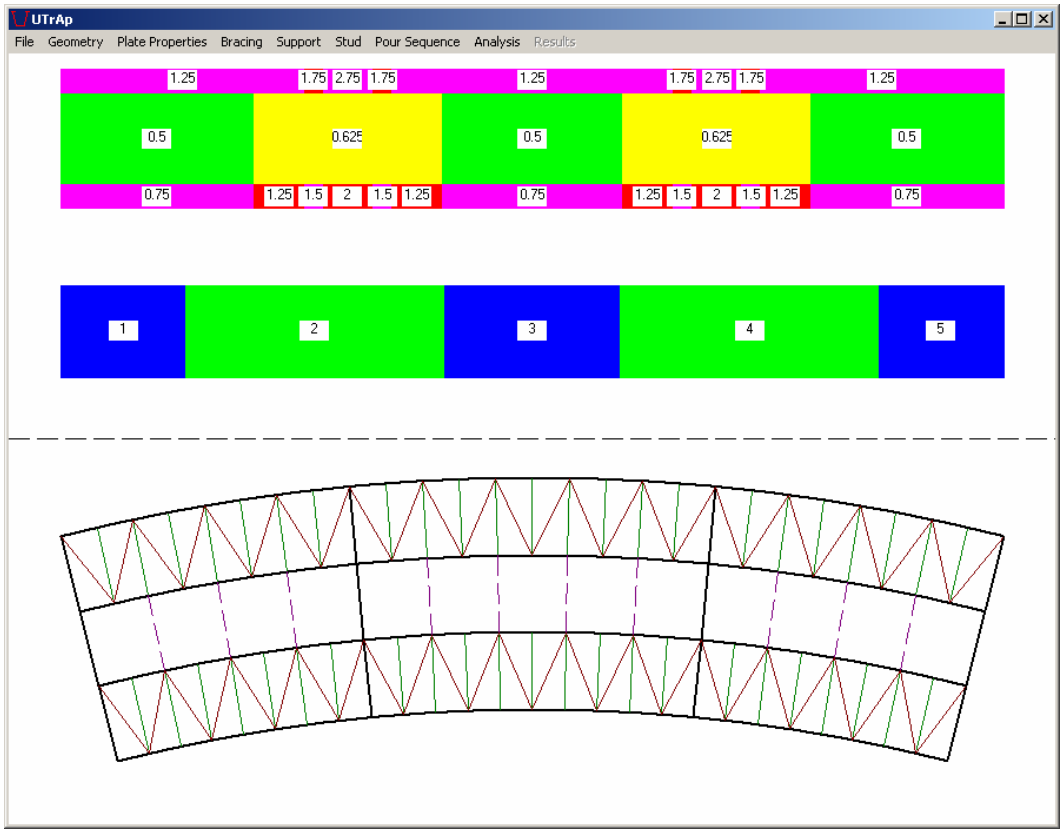

Figure 2.5 UTrAp Graphical User Interface (GUI)Main Form

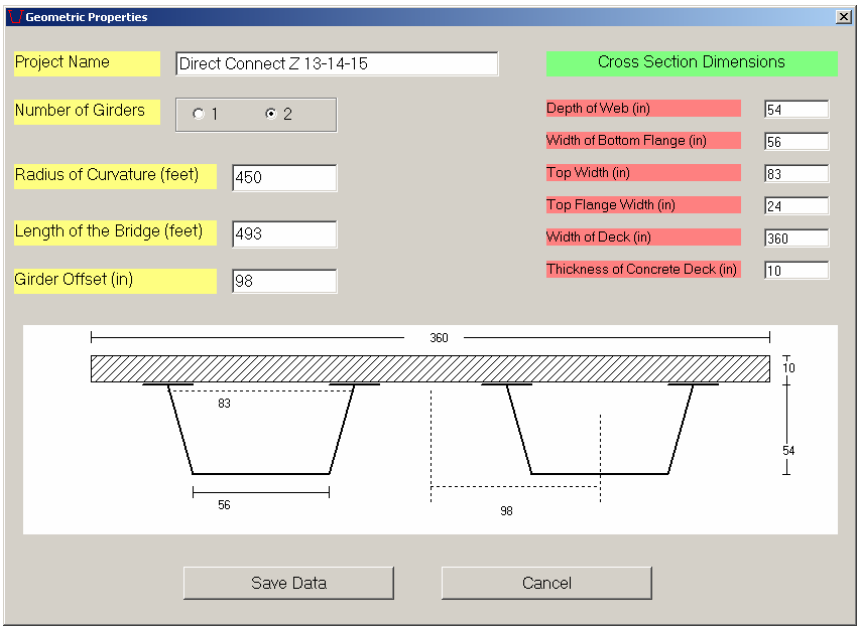

Figure 2.6 UTrAp Graphical User Interface (GUI)Showing Bridge Cross-Section

The GUI allows users to define the plate properties for all webs and flanges including web stiffeners, and these properties can vary over the length of a bridge. Users can also define top lateral, internal, and external bracing members. Any number of supports can be defined so that simple and continuous girder systems can be analyzed.

UTrAp is intended to perform both linear analyses and linearized buckling analyses of straight or curved steel trapezoidal box girder bridges under construction loading. The program is able to model the partially-composite behavior due to concrete curing during the bridge deck casting sequence. UTrAp is limited to elastic analyses, and it does not account for nonlinear material behavior. There are no limits on material stresses in the girder, and therefore care must be taken by the designer to ensure that the bridge remains elastic under the given loading.

While commercially available finite element software can perform the same computations that UTrAp performs, such software packages are usually not used in practice by design engineers. Aside from the complications noted above involving the time and effort needed to generate a suitable mesh, such software packages are relatively expensive. As such, many design firms avoid the use of such programs. UTrAp offers several distinctive advantages, as an alternative to such programs. First, its GUI is tailored for the analysis of curved box girder bridge systems, and it is possible to set up a problem within a very short amount of time. Second, the program has been validated against measured field data and other FEA software, and the results provided by the program accurately depict the response of the bridge system being analyzed. Third, UTrAp is available for free and can be downloaded from the website

http://www.ce.utexas.edu/prof/williamson/utrap2.htm. This website contains a detailed User's Manual with a worked example to allow users to become familiar with the program. The User's Manual also provides more general background information about the program development as well as the capabilities and limitations of the software. Because of these features, UTrAp allows engineers a viable alternative to less rigorous methods of analysis that may not accurately compute bridge behavior during the critical construction stages. The grid analysis approach can and should be used for initial member sizing and detailing, and to check the safety of the bridge in-service. More detailed analyses should be carried out when evaluating the suitability of a candidate final design with regards to critical construction stages and the associated stresses in internal and external bracing systems.

Chapter 3

Top Flange Lateral Truss

3.1 Introduction

Trapezoidal box girders are ideal structural shapes in curved bridge applications due to the large torsional stiffness. However, while the hardened concrete creates a closed box in the finished bridge, during transport and erection the steel girder is an open section that is relatively flexible in torsion. To improve the torsional behavior during construction, a top flange lateral truss is incorporated such as the one shown in Figure 3.1.

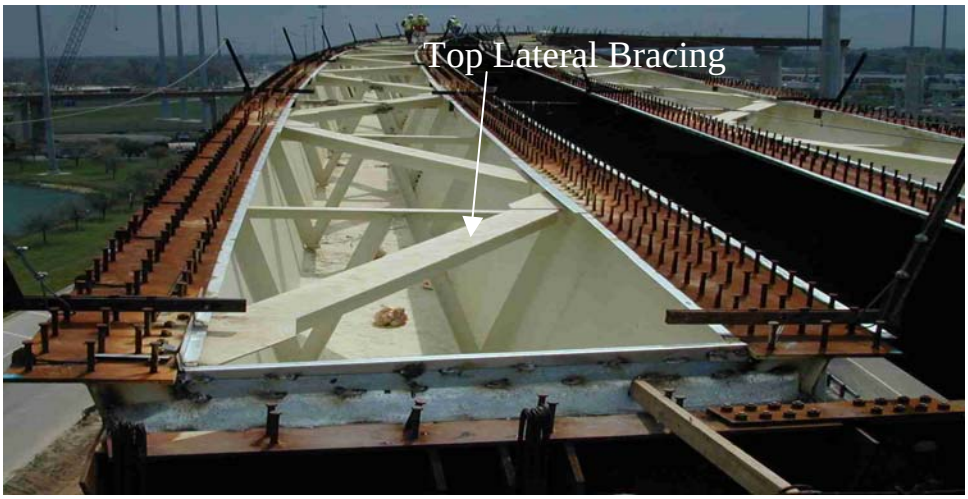

Figure 3.1 Top Flange Lateral Truss

The geometry of the top flange lateral truss system plays an important role in the behavior of the truss. While there are a variety of truss systems that might be employed, the most widely used system is the Warren truss shown in Figure 3.2a in which a single alternating diagonal is utilized. Another single diagonal truss system that has been proposed is the Pratt truss shown in Figure 3.2b (AASHTO 2007). The proposed Pratt truss layout is an attempt to minimize the weight of the truss; however such endeavors generally require extensive modeling that considers many load stages during construction and can be quite complicated. Another truss layout that has been used is the X-type truss shown in Figure 3.2c. Although equations will be presented for all three truss systems, much of the past research has focused on the Warren truss shown in Figure 3.2a and therefore the design procedures for that system will be the most comprehensive. The last section of the chapter includes a discussion of the benefits and negatives of the truss systems depicted in Figure 3.2.

The primary role of the top flange lateral truss is to improve the torsional stiffness as well as preventing spreading of the top flanges due to the sloping of the webs. For moderately curved

boxes, the resulting top flange truss will have enough strength and stiffness that stability issues are generally not a problem. However, for relatively straight girders the primary stability bracing is provided by the top flange truss. Failures such as the Marcy Pedestrian Bridge occurred due to the lack of a top flange truss, which resulted in lateral torsional buckling of the girder during placement of the concrete deck. Although the Marcy Pedestrian Bridge did have closely spaced internal K-frames, the torsional flexibility of the open box girder was inadequate to support the wet concrete load. The stability bracing requirements for box girders have been discussed by Chen, Yura and Frank (Chen et. al January 2002).

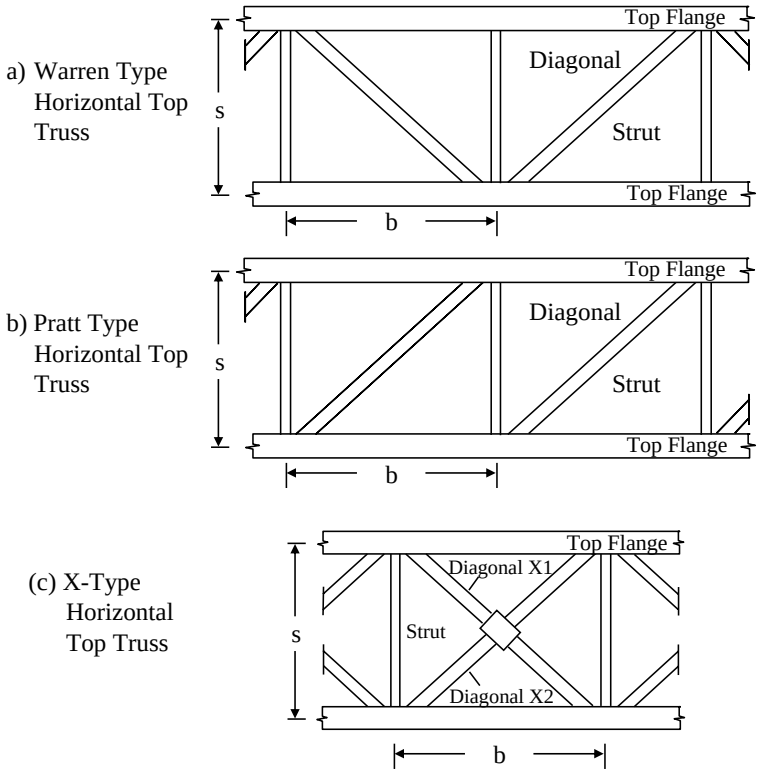

Figure 3.2 Geometries for Top Flange Lateral Trusses

Although the primary function of the top flange lateral truss is to increase the torsional stiffness of the girders, from a behavior perspective, the trusses can also develop significant forces due to vertical bending of the box girders. A difficult aspect in the analysis of horizontally curved box girders is the combination of bending and torsion under general applied loads.

A three-dimensional finite element analysis that models the top flange truss system can capture all the force components; however grid models depend on the user to recognize the effects of both torsional and flexure on the bracing systems. A method of accounting for box girder bending on the truss forces was presented by Fan and Helwig (1999) [also summarized in

Fan, 1999, Helwig and Fan (1999)]. The method depends on separating the bending and torsional solutions and then combining the results using the principle of superposition.

The remainder of this chapter focuses on hand solutions for calculating design forces in the top flange truss. A discussion of brace forces from torsion will be presented first followed by the effects of the sloping webs on the strut forces. An overview of forces induced from box girder bending is then covered. The final section of the chapter discusses top flange truss detailing issues and suggestions to aide the designer in establishing the basic geometry of the top flange truss.

3.2 Design of Top Flange Truss for Torsion

Analytical models employed by grid analyses do not directly model the top flange lateral trusses. Instead, an approximate torsional analysis of a quasi-closed box girder is usually performed using the Equivalent Plate Method (EPM) developed by Kollbrunner and Basler (1969). According to the EPM, the top lateral truss system is treated as a fictitious plate so that the torsional properties of the box can be approximated during the structural analysis using the following expression:

$$K_T = \frac{4A_0^{\,2}}{\sum_i b_i / t_i} \qquad (3.1)$$

where, A_0 is the area enclosed by the box measured to the center of the plate elements, and b_i and t_i in the summation are the respective width and thickness of the ith plate that make up the cross section.

The equivalent thickness of the fictitious plate was developed by Kollbrunner and Baslar (1969) for various truss systems using energy methods. The expressions for the equivalent thicknesses of the common truss systems used in trapezoidal box girders are given in Figure 3.3 (Kollbrunner and Baslar 1969).

t* = equivalent plate thickness;
E = Modulus of elasticity (29000 ksi for steel);
G = Shear modulus (11200 ksi for steel);
s = panel length (spacing between struts);
b = strut length (width between flanges);
L_d = diagonal length $= \sqrt{s^2 + b^2}$;
A_d= area of diagonal;
A_s= area of strut;
A_f= area of girder top flange (one flange).

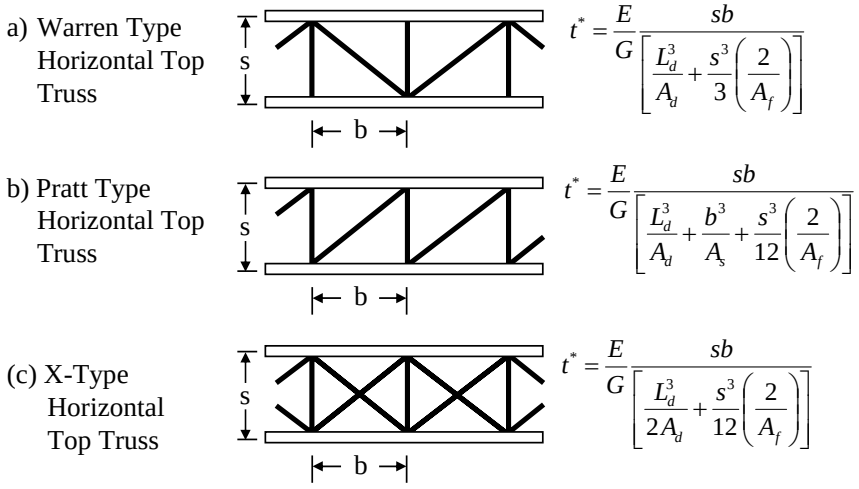

Figure 3.3 Expressions for Equivalent Thickness of Top Flange Truss System

The resulting torsional properties are used in the structural analysis to determine the torsional moments in the girders. Once the distribution of torsional moment is known, the shear flow, q, can be determined and can be used to determine the forces in the top flange lateral truss. For single-celled box girders, the expression for the shear flow is given by the following expression (Kollbrunner and Basler, 1969):

$$q = \tau t = \frac{M_T}{2A_0} \qquad (3.2)$$

where, τ is the shear stress, t is the thickness of the plate under consideration, M_T is the torque a the particular location, and A_0 is as defined in Equation 3.1.

The shear flow acting on the fictitious plate is then transformed into diagonal member forces in the lateral truss as demonstrated in Figure 3.4b and 3.4c. The nature of force (compression or tension) is important with regards to superimposing the torsionally-induced force with the other force components that will be discussed subsequently. The torsional loading in the Warren truss leads to alternating tension and compression in the diagonals along the length. In the X-type truss, the torsional loading causes one diagonal to be in tension while the other diagonal is in

compression. For designing the compression diagonal, the unbraced length can be taken as half the diagonal length provided the two diagonals are connected at the middle.

Although the Warren truss is shown in Figure 3.4b, the same expression would be used for the Pratt truss except the forces would generally be all tension provided the diagonals are oriented properly. In regards to the orientation, the designer must be very careful to consider all possible construction loads so that the diagonals do not experience compression under certain stages which may lead to buckling of the member.

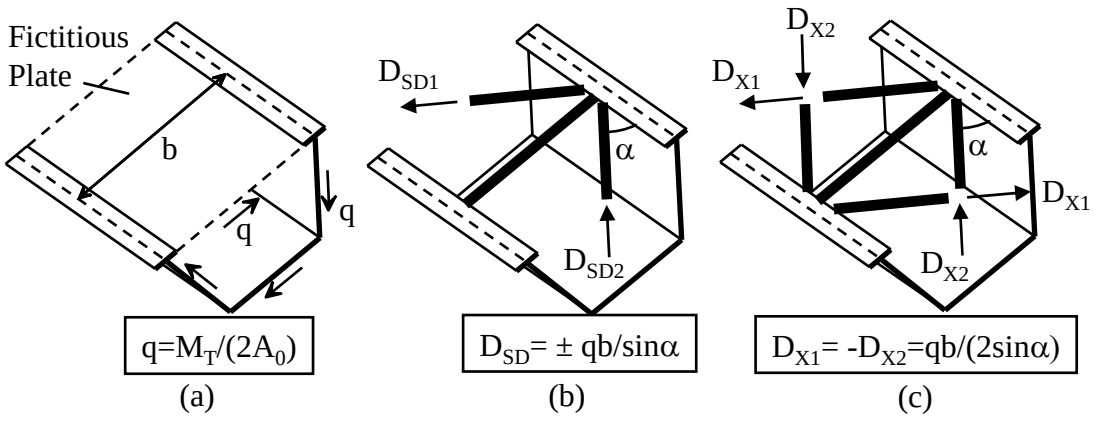

Figure 3.4 Diagonal Brace Forces Due to Torsion According to the Equivalent Plate Method (EPM)

Because the torque typically varies along the girder length, the struts in the top flange truss should be designed for the unbalanced force between adjacent panels in the Warren and X-type layout. For example, considering the diagonals for the truss in Figure 3.4b, the forces in the two adjacent panels can be taken as D_{SD1} and D_{SD2}. The torsional component of the design force in the strut would be the unbalanced horizontal component given by the following expression:

$$F_{T\,Strut} = (D_{SD1} - D_{SD2})\sin\alpha \qquad (3.3)$$

While the torsion-induced components in the struts were not specifically discussed in Fan and Helwig (1999), the values were taken into consideration in the equations. A short discussion on the torsional behavior of the struts was provided in Helwig et. al 2004. A more detailed discussion is provided in Kim and Yoo (2006).

As with the torsional component of the diagonal force from above, the nature of the strut force is important for the purposes of superimposing this torsional force with other force components that will be discussed subsequently. In a Pratt truss the strut force is the full value of *qb* and is compressive.

3.3 Effect of Sloping Webs on Strut Forces in Horizontal Top Flange Truss

The sloping webs of the trapezoidal girders also induce a lateral load component on the top flange. This lateral load component causes additional lateral bending stress as well as axial forces in the lateral struts of the top flange truss. The struts for the top flange truss are typically designed to carry the horizontal component due to the sloping webs. Historically, some past design aides (Highway 1982, and Four 1997) provided recommendations for the design of the struts for the lateral load component as well as accounting for lateral bending of the flanges between the struts. One of the assumptions in these past recommendations for evaluating the required forces in the struts and the lateral bending stresses in the top flange is that the top and bottom flanges each carry half of the horizontal web components of the applied load. Based on this assumption, the half acting on the bottom flange does not generate any top flange lateral bending stress or forces in the struts. While this assumption would be relatively accurate for the girder self-weight, the sloping web component from external loads from sources such as the fresh concrete deck must be resisted by the top flange lateral truss. This can be demonstrated by considering a free body diagram of the top flange with an externally applied distributed load of W/2 applied to each flange. Figure 3.5 demonstrates the transformation of the vertical load into a web shear and a horizontal component, p (force per unit length). For a truss panel length of s, the recommended design tensile force for the struts is therefore equal to ps. The maximum lateral bending moment in the top flanges due to the horizontal component is therefore equal to $(ps^2)/12$, assuming the flange behaves like a continuous beam supported at the strut locations (Fan 1999, Helwig and Fan 2000). The tensile component in the struts can be superimposed on the torsional components discussed in the last section as well as other components from vertical bending and box girder distortion that are discussed in the next section and the following chapter.

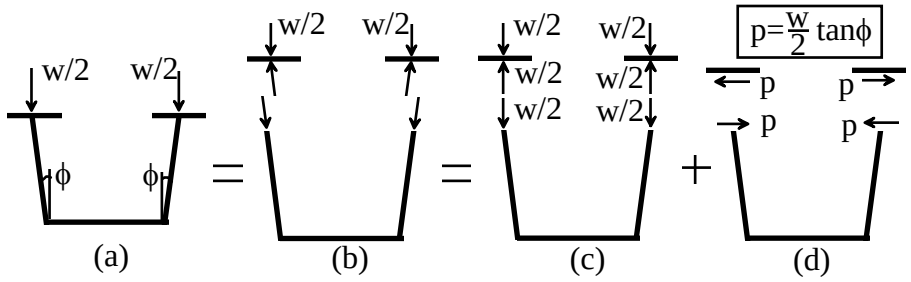

Figure 3.5 Horizontal Component of Applied Loads on the Top Flanges

3.4 Design of Top Flange Truss for Box Girder Flexure

In addition to torsionally-induced forces, the top flange truss also develops forces due to vertical bending of the box girder. These force components are generally undesirable since the primary purpose of the lateral truss is for torsional stiffening. The cause of these forces is demonstrated in Figure 3.6, which shows a box girder with a horizontal truss located near the top

flange. The distribution of longitudinal bending stress is also depicted in the figure. Due to strain compatibility between the top flange of the girder and the truss, forces will develop in the top truss as a result of vertical bending of the girder.

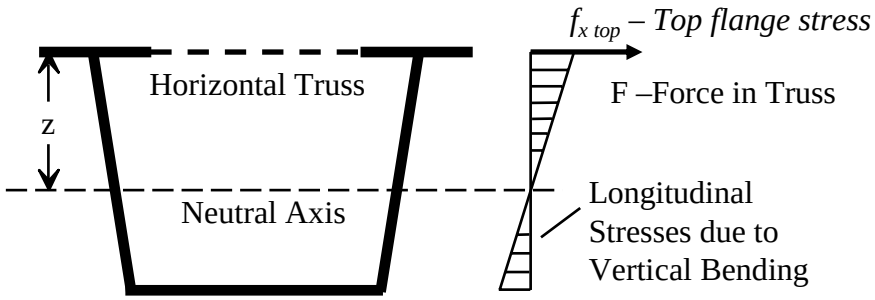

Figure 3.6 Box Girder Vertical Bending Stresses

The behavior of the top truss to vertical box girder bending for the Warren and X-type systems have been discussed in past literature (Fan and Helwig 1999, Fan 1999, Helwig and Fan 2000). Equations for predicting the truss forces induced due to vertical bending of the box girder are summarized in Figure 3.7. The Warren truss layout also results in a lateral load on the flanges that cause the flange stress denoted by $f_{L\ bend}$ in the figure. Considering the Warren truss layout, although the forces due to torsion tend to alternate tension and compression, the forces due to bending have the same state of stress as the top flange box girder stresses, $f_{x\ top}$. As mentioned earlier, the state of stress for the bending-induced component in the top flange truss should be maintained for the purposes of superposition of the stress effects from various sources such as torsion, bending, and box girder distortion.

The expressions given in Figure 3.7 were developed for the specific case of internal K-frames positioned in every other panel, which is a spacing of *2s*, where *s* is the spacing between the struts of the top flange truss. Bending induced forces in the top flange truss are sensitive to the spacing between the internal K-frames. When internal K-frames are spaced at every panel point of the top flange truss (spacing of *s*), the bending induced forces are actually larger (Li 2004, Helwig et al. 2004). As covered in the next chapter, the recommended layout of the internal K-frames is therefore at a spacing of *2s* (every other panel point). At the truss panel points between the internal K-frames only a strut is provided.

D_{bend} = bending component in diagonal
S_{bend} = bending component in strut
$f_{x\ top}$ = top flange bending stress in panel
s =panel length (spacing between struts)
α = Angle between diagonal and flange
L_d = diagonal length
b =strut length (width between flanges)
A_d, A_s = respective area of diagonal or strut
b_f, t_f = respective width and thickness of girder flange
$f_{L\ bend}$ = lateral bending stress in girder top flange

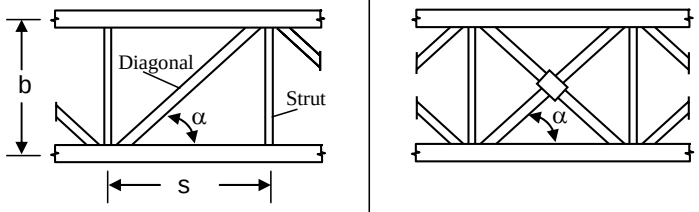

$$D_{bend} = \frac{f_{xTop} s \cos\alpha}{K_1}$$

$$K_1 = \frac{L_d}{A_d} + \frac{b}{A_s}\sin^2\alpha + \frac{s^3}{2b_f^{\,3} t_f}\sin^2\alpha$$

$$S_{bend} = -D_{bend}\sin\alpha$$

$$f_{L\ bend} = \frac{1.5s}{b_f^{\,2} t_f} S_{bend}$$

$$D_{bend} = \frac{f_{xTop} s \cos\alpha}{K_2}$$

$$K_2 = \frac{L_d}{A_d} + \frac{2b\sin^2\alpha}{A_s}$$

$$S_{bend} = -2D_{bend}\sin\alpha$$

Figure 3.7 Equations for Bending Induced Forces in Top Flange Truss

The authors are aware of no work reported on the bending behavior of box girders with the Pratt layout. Since a relatively limited amount of study has been conducted on the Pratt layout, the behavior to bending induced forces has not been documented. While it may seem the above referenced expressions should be directly applicable, this conclusion is not possible without significant parametric investigation. A conservative estimate of the bending induced forces for the Pratt layout could probably be obtained by using the equations for the Warren layout. However, the use of the Pratt layout is strongly discouraged unless a three-dimensional finite element analysis is conducted on the system and even then the engineer must carefully consider the entire construction procedure.

3.5 Top Flange Truss Details

3.5.1 General Detailing

Several factors should be considered in establishing the geometry for the top flange truss. The number of panels that are used as well as the orientation of the diagonals can have a significant effect on the efficiency of the design as well as the performance of the girder system. In specifying the number of panels along the span length, the engineer should try to keep the angle of the struts, α (defined in Figure 3.7), within the range $35° < \alpha < 50°$. The upper limit on this range is related to economics since larger values of α will lead to more panels which results in more connections and larger fabrication costs. The lower limit on this range is related to the compression behavior of diagonals from both torsional and vertical bending. With a smaller angle of inclination, the diagonals become relatively long and therefore possess a lower buckling capacity. In general, diagonals with orientations outside of the range $35° < \alpha < 50°$ are inefficient and should be avoided.

Structural T-sections are often used for the diagonals, while angles are commonly used for the struts. For practicality of the connections and safety of the construction workers, the T-sections should be oriented with the stem pointing downwards. The construction personnel often must walk on these members during erection and early stages of construction. In addition, the stem should be pointed downward to avoid clearance issues with the metal deck forms. In detailing the connections for the diagonals, care should be taken not to employ excessively thick connection plates or shims that will increase the eccentricity of the connection. The thickness of the connection plate should be approximately equal to the thickness of the WT flange. Diagonals in compression should be treated as a beam-column with a moment equal to the design axial force acting at an eccentricity equal to the distance from the centroid of the T-section to the plane of the connection. Provided the WT flanges are wide enough, better economy in the connection can be achieved by bolting the diagonal directly to the top flange. In addition to reducing the fabrication costs by eliminating the connection plate, this connection results in less eccentricity. However, in some cases it can be difficult to fit an adequate number of bolts onto the flange in the positive moment region and connection plates may have to be provided.

As shown in Figure 3.8, the strut for the top flange truss also serves as the top member of an internal K-frame if one is provided at the panel point. To avoid congestion at the intersection of the struts and the diagonals, some designers connect the strut to the web stiffener at an eccentricity denoted as *e* in Figure 3.8. This eccentricity generally doesn't have too significant of an effect on the performance of the top flange truss; however the eccentricity should be limited to a maximum value of 3 or 4 inches. In many cases, dropping the strut due to concerns about congestion between the diagonals and the struts is unnecessary due to the inclination of the diagonals and the length of the connection. In cases where the Pratt truss geometry might be considered, the eccentricity in the strut can lead to relatively poor load paths as is discussed in the following pages.

3.5.2 Diagonal Geometry (Warren and Pratt Truss Layouts)

For a given design force, the stability requirements of compression members require larger member sizes than for equally loaded tension members. Proper orientation of the diagonals can lead to more efficient designs with regards to sizing members for compression. Figure 3.9 shows the plan view of the suggested layout near the end panels of the top flange truss. The maximum top truss diagonal forces to resist torsion due to girder curvature will occur at the ends of the span. To minimize the required member sizes, the diagonals in these panels have therefore been positioned so that torsion causes tension in the diagonals. The second panels in from the supports are then the critical panels for compression.

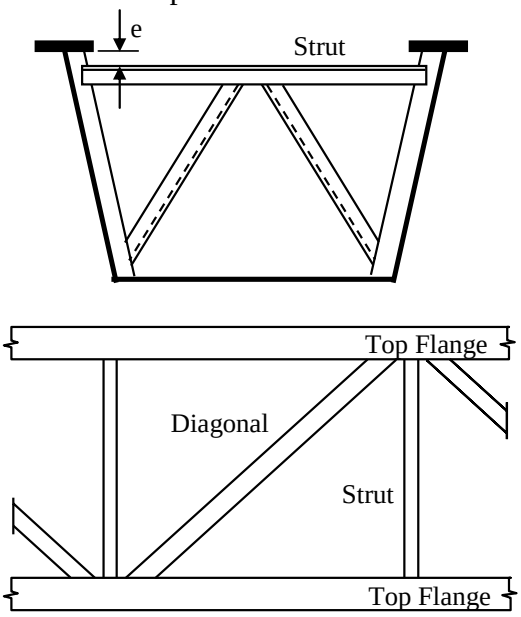

Figure 3.8 Potential Eccentricity in Strut Connection

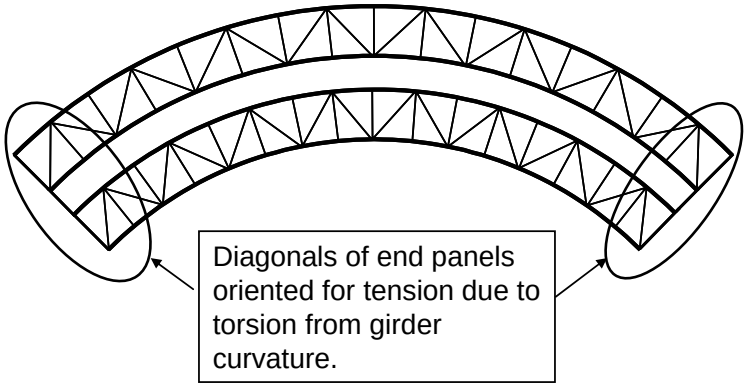

Figure 3.9 Orientation of End Diagonals so Torsion Produces Tension in Diagonals

To optimize the layout of the top flange truss and avoid compression in the diagonals the Pratt truss geometry that was shown in Figure 3.2b has been proposed (AASHTO 2007). The idea behind the Pratt truss is to orient the diagonals so that they are only subjected to tension, thereby getting smaller member sizes. Figure 3.10 shows a typical layout that would result in a simply-supported curved box. A sketch of a typical distribution of torque is also shown in the figure. With simply supported boundary conditions the location where the torsional diagram changes sign is relatively simple to predict and therefore the location to flip the orientation of the diagonal so as to avoid compressive forces from the torque is readily apparent. However, in the more common uses of curved box sections the girders are continuous over multiple spans. In these applications, predicting the optimum layout of the diagonals is much more complicated. The designer must carefully consider the many stages during erection and casting of the concrete bridge deck to evaluate the safety of the top flange truss with respect to potential diagonal compression. The distribution of torque and bending moment can vary significantly throughout the construction process and some of the diagonals will likely experience compression during these phases. As a result, engineers should pay extra attention to analyzing for the proper layout and critical design forces when considering using the Pratt layout for the top flange truss.

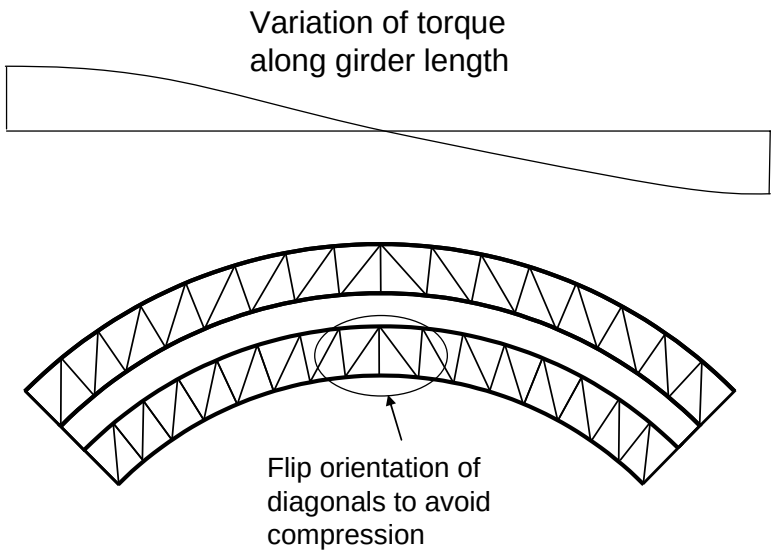

Figure 3.10 Diagonal Orientations in Pratt Truss Layout

One other drawback to the Pratt layout of the top flange truss is the complicated load path that results along the girder length when compared to the Warren truss geometry. In the Pratt layout, the struts become major members in the load path along the girder length. While the struts in the Warren truss layout are important members, their primary role is in transferring loads locally within two adjacent panels. The load paths are depicted in Figure 3.11 for the two truss systems. In the Pratt truss in Figure 3.11a, the strut must handle the entire lateral component of the diagonal force induced from torsion. Depending on the connection detail that is used for the strut, the resulting load transfer may have to follow a relatively indirect path. With an eccentric connection such as the one depicted in Figure 3.8, forces from the diagonal in the Pratt truss would be transferred into the web/stiffener of the girder, down to the strut and across the girder, back up the web/stiffener of the girder and into the diagonal of the adjacent panel. In the Warren truss layout depicted in Figure 3.11b, the role of the struts at resisting torsional loads is primarily local in that they must handle the unbalanced load from the diagonals in the two adjacent panels.

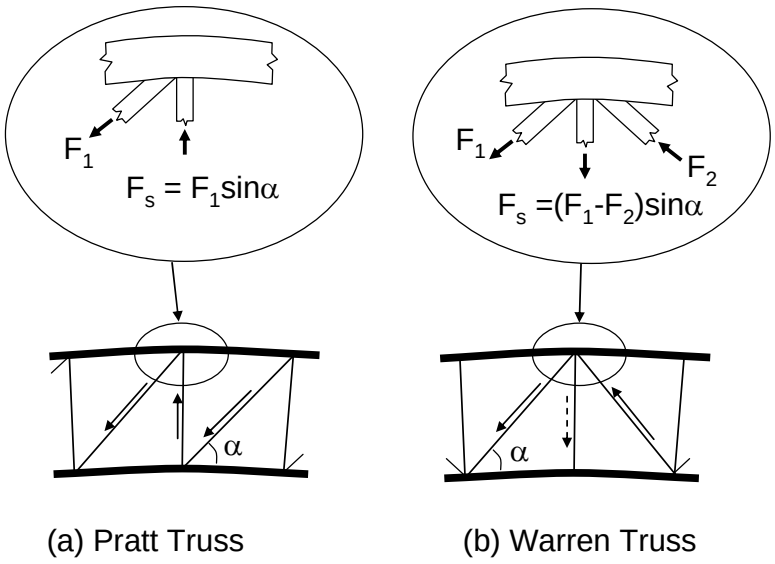

Figure 3.11 Role of Struts in Load Path of the Pratt and Warren Truss Systems

The purpose of the discussion of the Pratt truss geometry presented herein is not to necessarily discourage the use but instead to emphasize the necessity of carefully considering the loading stages so that a safe design results with good behavior. In general, the authors would not recommend employing the Pratt layout without a three-dimensional finite element analysis that considers the various load stages of the concrete placement.

3.5.3 Top Flange Truss Details in Girders with Skewed Supports

The design requirements of the top flange lateral truss for both torsion and bending are generally not sensitive to whether or not the supports are skewed or radial. However, the detailing of the truss can be affected. With skewed supports, the end panels of the top flange trusses of adjacent boxes may have to be irregular to the other panels; however the decisions on the final layout are mainly a function of geometrical considerations with several viable solutions.

While the design requirements of the truss are not affected too significantly due to the presence of skewed supports, the combination of the skew angle and the use of external K-frames can affect the performance and detailing of the top flange truss. External K-frames are often used in box girder system to control the relative twists of adjacent boxes and are discussed in detail in Chapter 5. In most situations, the forces that develop in the external K-frames are relatively small. With skewed supports, the forces in the external K-frame will generally be larger than for cases with radial supports and designers may want to consider modifying the top flange truss details. The reason for the larger external brace forces with skewed supports is because the external K-frame connects to the adjacent girders at different locations along the girder lengths. As a result the two ends of the cross-frame undergo different vertical displacements, which can lead to larger forces developing in the external K-frame.

Figure 3.12 shows a recommended detail that was presented and discussed in Li 2003 (Helwig et. al 2004). Two layouts are shown in the Figure with labels "Parallel Layout" and "Mirror Layout". In the parallel layout, the truss diagonals of the adjacent girders are parallel along the girder lengths in the respective panels. For example, in the first panels on the left of the plan view the strut connects the box girder interior top flange at the support to the exterior top flange at the end of the first panel. In the mirrored layout, the corresponding diagonal on the interior girder connects the exterior flange at the support to the interior flange at the end of the panel.

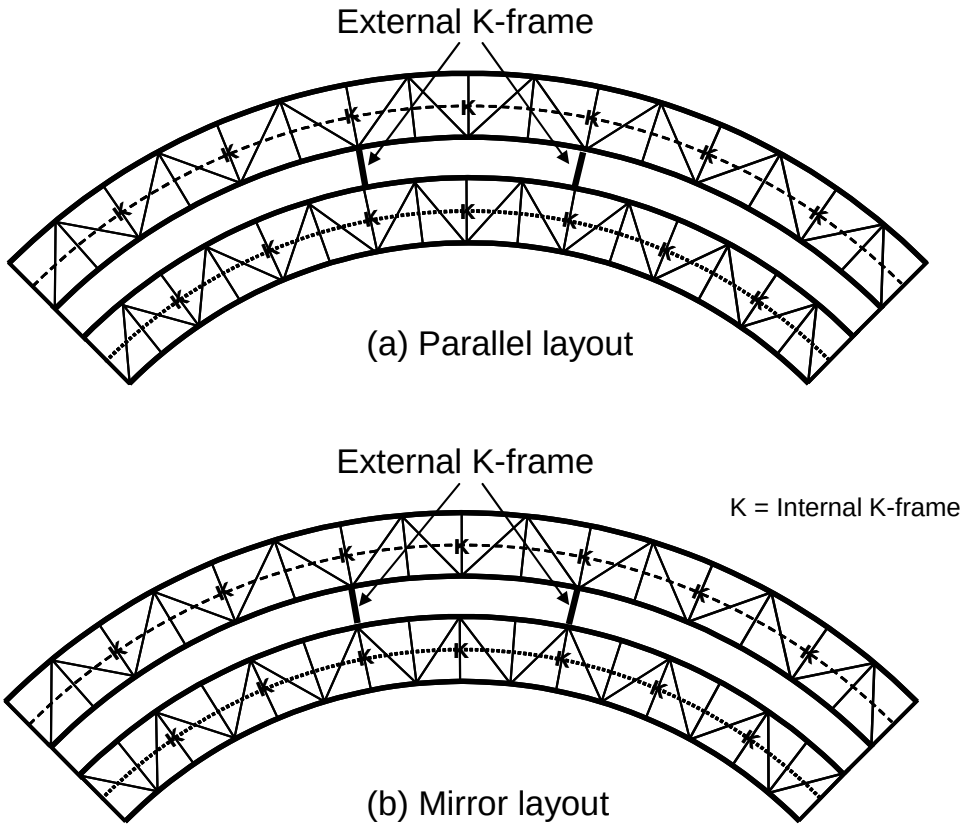

Figure 3.12 Parallel Versus Mirrored Layout of Top Flange Lateral Truss

The benefits of the mirrored layout can be seen by considering the region around the external K-frames as depicted in Figure 3.13. With the parallel layout, the external K-frame connects to the exterior girder at a location where the truss diagonals frame into the top flange while on the interior girder the truss diagonals do not restrain the flange with the external K-frame connection. The forces in the top strut of the truss/internal K-frame can therefore become quite large. In the mirrored layout, the top truss diagonals on both girders frame into the box girder flange at the location of the external K-frame help to distribute the force into the girder. The mirrored layout should generally be considered for girders with support skews exceeding

approximately 20 degrees. An alternative to the mirrored layout might be to add an additional diagonal to either one or both of the panels at the external K-frame location thereby forming X-type top flange truss diagonals at these locations. The additional diagonal would therefore help to distribute the forces from the external braces to the girders.

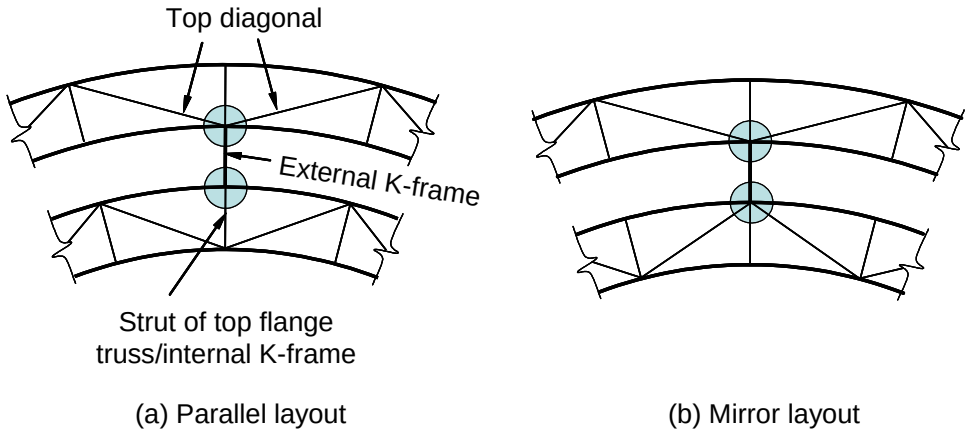

Figure 3.13 Parallel Versus Mirrored Layout Provides Better Restraints at External K-Frame Locations

Chapter 4

Internal K-Frames

4.1 Introduction

The primary role of internal K-frames is to maintain the shape of the cross section against torsional forces that tend to distort the shape of the box girder. Box girder distortion is generally caused by torsional forces that are not distributed to the elements of the girder cross-section in proportion to the St. Venant torsional stresses. This chapter outlines the design requirements for internal K-frames to properly control distortion and provides recommendations on detailing practices for the internal K-frames. A brief discussion of the nature of distortional components of the external loads is presented in the following section along with expressions that can be used to determine distortional induced forces in the internal K-frames. The final section of the chapter outlines detailing recommendations for the braces so as to result in predictable behavior of the girders in the final system.

4.2 Controlling Box Girder Distortion

The torsional stiffness of a cross-section consists of both warping and Saint Venant components; however the high torsional stiffness of boxes is primarily due to the large St. Venant component that results from a closed cross-section. Since the St. Venant term dominates the torsional stiffness, torsional warping stresses in boxes are usually relatively small (Kollbrunner and Basler 1969). However, depending on the distribution of the applied torsional loads, the cross-section of a box girder may distort from its original shape. This distortion of the cross-section can lead to significant warping stresses, which are in addition to torsional warping stresses. Warping stresses that develop as a result of distortion of the cross-section are appropriately referred to as distortional warping stresses. While torsional warping stresses in box girders may be relatively small, without proper bracing distortional warping stresses can be quite significant.

Box girder distortion is usually controlled by internal cross-frames that are spaced along the length of the girder. Forces develop in these cross-frames and other bracing members due to the distortion of the box section. Before expressions are presented for the distortion-induced brace forces in the cross-frames, an overview of how external loads cause box girder distortion should be presented. Torsion in box girders is usually the result of either horizontal curvature of the girder or unbalanced gravity loading that results in an eccentricity of the load on the cross-section. Depending on the type of loading, the torque on girders can be visualized as either a horizontal or vertical couple as depicted in Figure 4.1. The M/R method that was discussed in chapter 2 results in an effective torque similar to that depicted in Figure 4.1a. In the cases of unbalanced gravity loading, the effective torsional loading can be idealized as shown in Figure 4.1b. In the case of eccentric loading, the full loading can be modeled as depicted in Figure 4.2 in which the gravity loading is divided into a pure flexural load plus a torque consisting of a vertical couple.

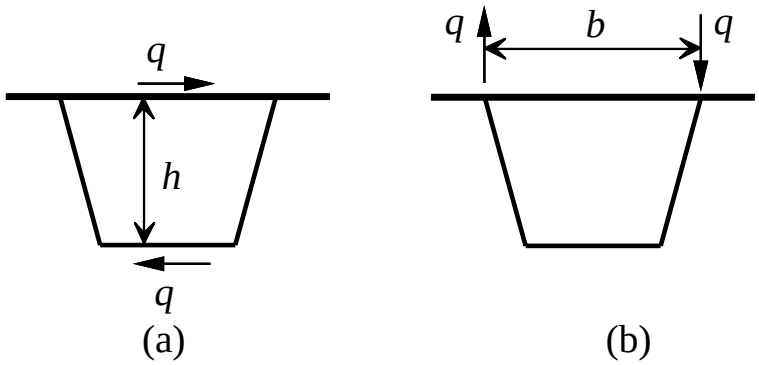

Figure 4.1 Representation of Torque on Box Girder

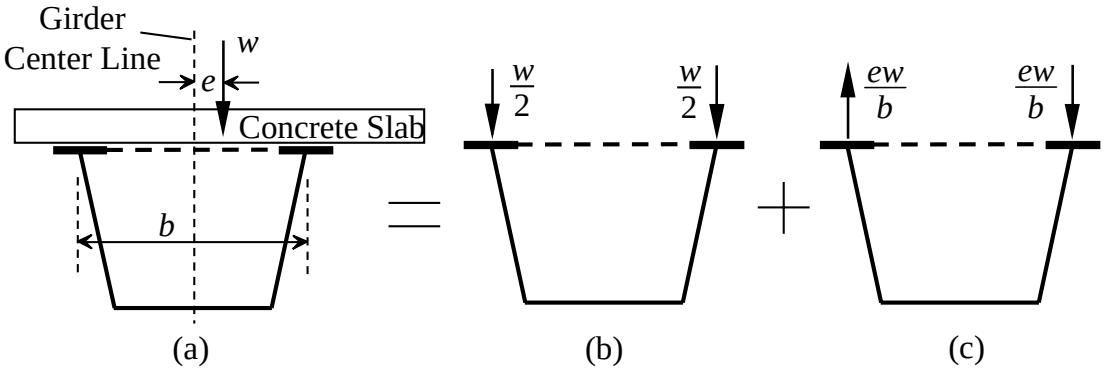

Figure 4.2 Effective Loading from Eccentric Gravity Loading

Cross-sectional distortion of box girders is induced by the components of the external torsional loads that are not directly distributed in proportion to a uniform Saint-Venant shear flow on the cross-section. All practical loading cases cause some form of box girder distortion since the load application is never distributed in proportion to the Saint-Venant shear flow. The load application can be divided into a torsional component and a distortional component. For example, depending on the nature of the applied torque, Figures 4.3 and 4.4 demonstrate resulting pure torsional and pure distortional components. Although the sections shown are rectangular in shape, the same basic principals apply to trapezoidal sections. The pure torsional components are distributed around the cross section in proportion to the St. Venant shear stresses. While the distortional components of the applied load yield zero net torque on the cross-section, these components can lead to large cross-sectional stresses if proper bracing is not provided. Although the resulting torque depicted in Figures 4.3 and 4.4 have the same net torque (m_T), the distortional components are in opposite directions. A distortional analysis therefore requires the separation of the distortional components from the applied torsional loads.

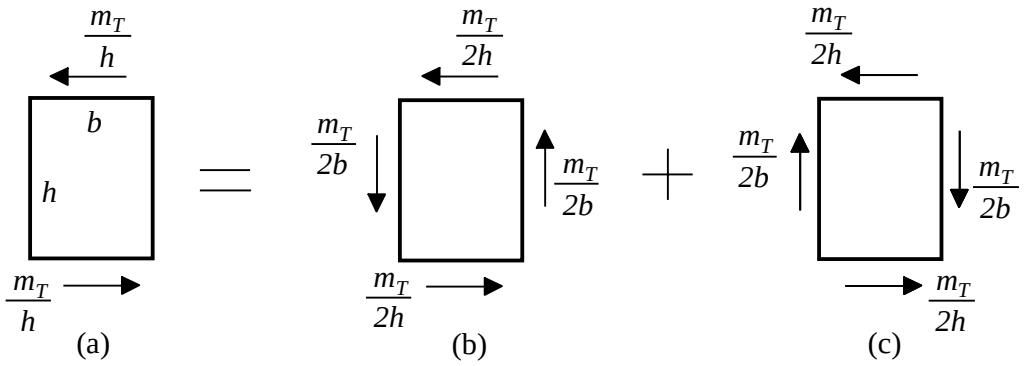

Figure 4.3 Pure Torsional and Distortional Load Components for Torque Resulting from Horizontal Couple

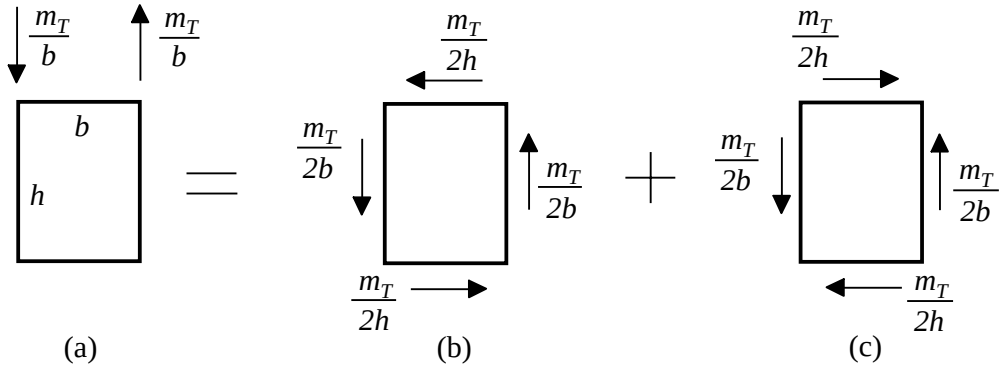

Figure 4.4 Pure Torsional and Distortional Load Components for Torque Resulting from Vertical Couple

Vlasov (1961) was the first to study distortion of box girders while investigating the torsional behavior of thin-walled beams with a closed cross-section. Dabrowski (1968) established a more rigorous theory when he developed the governing equation for box girder distortion and provided solutions for several simple cases. A discussion of the distortional components of torsional loads was provided by Fan and Helwig (Fan and Helwig 2002, Fan 2000). A detailed treatment of box girder distortion can be found in the above cited references from Vlasov and Dabrowski; however the presentation in this section will summarize the approximate methods presented in Fan and Helwig (2002).

Figure 4.5(a) shows the basic geometry of the box with the bottom flange width denoted as *a*, and the width between the top flanges as *b*. The distortional induced forces are depicted in Figure 4.5(b) as S and D for the respective struts and diagonals for the internal K-frame. As discussed above, the source of the torsional loading may come from either horizontal curvature or eccentricities in the applied loading. Fan and Helwig (2002) presented the following expressions for the distortional induced components in the struts and diagonals of the internal K-frames based upon the horizontal curvature and eccentric gravity loading:

$$D = \pm \frac{s_K L_{DK}}{2A_0}\left(\frac{M}{R} - \frac{a}{b} ew\right) \qquad (4.1a)$$

$$S = \pm \frac{s_K a}{4A_0}\left(\frac{a}{b}ew - \frac{M}{R}\right) \qquad (4.1b)$$

Where: D = distortional induced force in the K-frame diagonal;
S = distortional induced force in the K-frame strut;
s_K = spacing between internal K-frames measured along the girder length;
L_{DK}=length of the K-frame diagonal;
A_0=area enclosed by box=(a+b)/2h;
a and *b* = box girder dimensions as depicted in Figure 4.5a;
e = effective eccentricity of resultant distributed load;
w = distributed load (weight/ft.);
M= box girder bending moment; and
R = radius of horizontal curvature of box.

The *M/R* term in the parentheses is directed at the torsional effects of horizontal curvature while the *ew* term in the parentheses captures the effects of eccentric gravity loading. The plus/minus sign on the expressions indicates that the distortion induces tension and compression as indicated in Figure 4.5b. One diagonal experiences compressions while the other experiences tension. In the case of the strut, equal magnitudes of tension and compression are induced on either side of the two diagonals. Since the struts serve as members of both the internal K-frames and the top lateral truss, these members have torsional components from box girder bending, torsion, and distortion. The components due to torsional and bending are uniform across the strut while the distortional components have equal magnitudes of tension and compression as indicated by the plus/minus sign in Equation 4.1b. The distortional component can therefore be isolated from the bending and torsional component by averaging the magnitudes of the strut force on either side of the two diagonals.

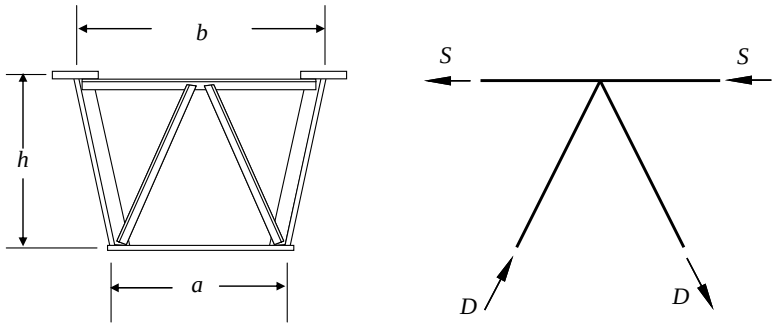

Figure 4.5 Strut and Diagonal Forces in Internal K-Frame

4.3 Detailing of Internal K-frames

The equations presented in the last section provide estimates of the distortion-induced forces in the internal K-frames as a function of the spacing between the brace points. The original derivation of the expressions was outlined in Fan and Helwig (2002) and the expressions had excellent agreement with parametric studies using FEA models of twin box girder systems.

The geometry that was utilized in the original study matched the internal K-frame layouts for box girders that had been encountered in the early 1990's. These girders had internal K-frames positioned at every other panel point of the top flange lateral truss as depicted in Figure 4.6. The plan view of a box is shown in Figure 4.6a with the labels *K* and *S* used to denote sections of the box girders at the panel points of the truss. At panel points with a *K*, an internal K-frame was provided as shown in Figure 4.6b while in cases with an *S*, only a top strut was provided as shown in Figure 4.6c.

By the mid to late 1990's, many of the box girder applications in Texas utilized internal K-frames at every panel point of the top flange truss. After the paper by Fan and Helwig (2002) was published, Fan discovered that the accuracy of these expressions was dependent on the geometrical layout of the cross-frames relative to the panel points of the top flange lateral truss. This finding was later confirmed by Li (Li 2004, Helwig et. al 2004) in a parametric study that considered several factors including top truss panel geometry, K-frame spacing, radius of curvature and several other parameters. The results clearly showed that positioning the internal K-frames at every other panel point produced better behavior than the current practice of using these internal K-frames at every panel point. Therefore, the authors recommend an internal K-frame spacing of every 2 panel points of the top truss.

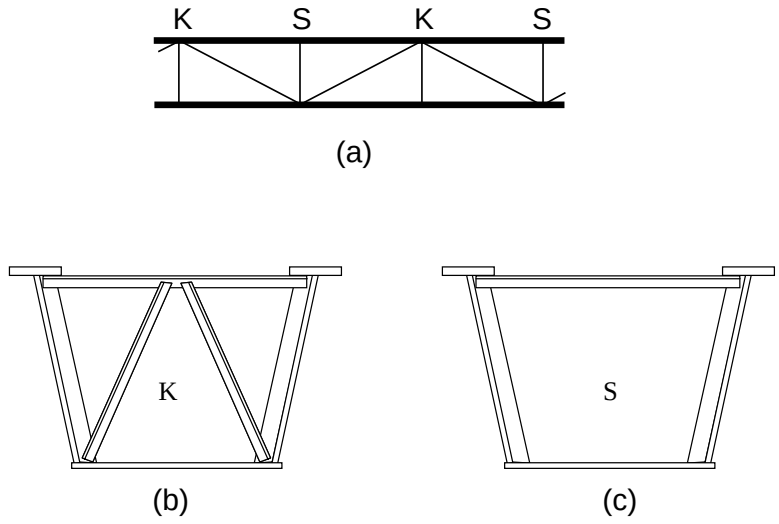

Figure 4.6 Girder Bracing Details at Top Truss Panel Points

Chapter 5

External Bracing for Box Girders

5.1 Introduction

Chapters 3 and 4 focused on bracing systems that are internal to the box girder. This chapter discusses the role and the design requirements for braces that are external to the box sections. The primary external bracing for the box girders consist of diaphragms that control the twist of the cross section. External diaphragms are always provided at the supports and may also be placed at intermediate locations along the length of the bridge. Solid plate diaphragms are typically provided at the supports while the intermediate diaphragms usually consist of K-frames. Plate diaphragms at the supports are critical members for torsional equilibrium of the box girder system. The external K-frames that are positioned along the bridge length may often not be necessary for strength of the girders but play an important role controlling relative twist of the adjacent box girders. The following two sections of this chapter provide a discussion of the behavior and design requirements for these two critical bracing systems. External K-frames will be covered first followed by solid plate diaphragms.

5.2 External K-frame Braces

The primary role of the intermediate external diaphragms is to control the relative deformation between adjacent girders during casting of the concrete bridge deck. Figure 5.1 depicts the effects of relative deformations without external K-frames versus the better control achieved when the K-frames are included as shown in Figure 5.2.

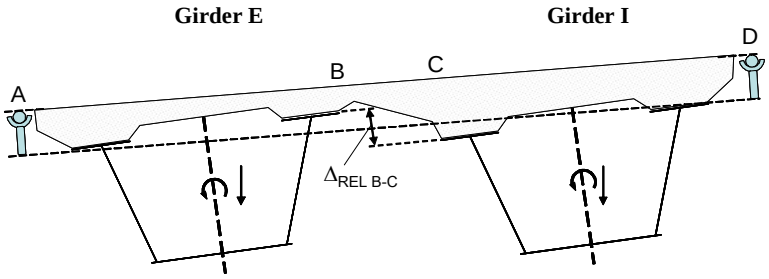

Figure 5.1 Relative Deformation Between Adjacent Girders Result in Variability in the Slab Thickness

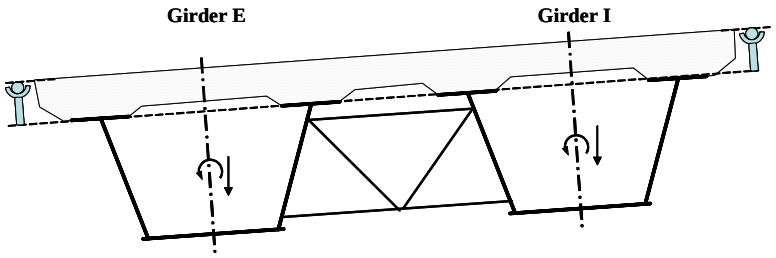

Figure 5.2 Intermediate Braces Help Control Girder Twist to Achieve Better Uniformity in the Slab Thickness

The deformations depicted in Figure 5.1 are exaggerated; however a small amount of relative deformation between adjacent box girders can have detrimental effects on the slab durability. The critical regions for the slab deformations are generally at the top flange tips labeled B and C in Figure 5.1 since the relative movement of these points can have detrimental effects on the slab geometry. The concrete finishing machine is supported on rails at points A and D at the edge of the bridge and the resulting top of the slab will be finished along parallel to a straight line between these two screed rails. Because the steel mat in the slab is tied together and supported on the formwork, the twist of Girder E in Figure 5.1 can lift the mat of steel and result in a significant reduction in the concrete cover of the reinforcement in the top lf the slab. The reduction in concrete cover can lead to durability problems in the slab, resulting in costly rehabilitation costs during the service life of the bridge. The presence of intermediate cross-frames helps to control the relative deformation between adjacent girders, thereby resulting in better uniformity in the slab thickness across the width of the bridge.

Good control of the slab thickness can often be achieved with bracing at only a few intermediate points between the supports. Three-dimensional finite element analyses have shown that in many situations diaphragms at a few locations along the girder length are often just as effective as several cross-frames along the girder length (Li 2004, Helwig et. al 2004). The cross-frames near the middle of the span are generally the most effective at controlling the relative girder twist. Therefore, engineers may be better served by skewing the cross-frames towards the middle of the span instead of spreading the braces out equally along the bridge length. Although the deformations often don't differ substantially with the addition of several braces, the forces induced in the intermediate cross-frames will be smaller as more braces are added. However, the forces in the intermediate cross-frames from the construction loading are often relatively small. With skewed supports, the forces in the cross-frames do become larger; however unless the support skew becomes large (greater than approximately 30 degrees), the forces can often be handled with "typical" size members.

External intermediate K-frames are primarily needed on horizontally curved girders. In straight girders, if diaphragms are provided at the supports and a top flange lateral truss is utilized, the girders are very stiff and no intermediate external diaphragms are required. Two exceptions to this case would be if a large unbalanced load (ie. Large torque) is applied or if the supports have significant skew. The problem with the large support skew is that the ends of the girders may tend to twist due to the angled diaphragm. The twist at the support results in a rigid body rotation of the girders that can result in problems with the uniformity in the slab thickness as outlined earlier. Most practical applications of straight girders do not need

external bracing. The following two subsections will cover analysis approaches and approximate design expressions.

5.2.1 Analysis Approach for Intermediate External Diaphragms

The treatment of the external braces in the structural analysis as well as the accuracy of the resulting forces depends heavily on the analysis method that is used. If a three-dimensional finite element model is utilized, the braces can be modeled relatively accurately and the member forces can be obtained directly from the analysis. However, incorporating the external K-frames into a grid model poses a complicated geometrical problem. Although the internal and external K-frames are trusses made up of several members, the grid models often treat these braces as a line element that spans between the centerlines of the adjacent girders. Therefore estimating the stiffness of these external braces can create a difficult problem. In addition, the analytical estimates of the intermediate diaphragm moments from a grid model may often be of questionable accuracy.

As mentioned in Chapter 2, another possible analysis approach is to designate the intermediate external K-frames solely as members to help control the constructability of the slab. With this approach, the analysis would be carried out only modeling the girders and solid diaphragms at the supports. The girders and support diaphragms would therefore be sized to support the entire load. This will often result in larger member sizes for the top flange lateral truss, when compared to an analysis that includes the external braces; however the economics of the top flange truss should not change too dramatically. The cost of the top flange truss is mainly related to fabrication costs, which are often primarily a function of the number of pieces required to fabricate. Increasing the size of a member by a few pounds per foot should not have too large of an impact on the design economics, however the behavior and safety of the design are much easier to predict with this approach. Although they are not included in the analysis, the intermediate external K-frames are provided to ensure better uniformity in the slab thickness. As mentioned above, a few external cross-frames skewed near the middle of the span often provide excellent control over the relative twist between adjacent girders. Although "typical" sizes can probably be used on these members, approximate design expressions are developed and discussed in the following two subsections.

5.2.2 Required Spacing of Intermediate External K-frames

The approximate expressions that are outlined in this subsection are for use in determining how many intermediate cross-frames are needed. The following subsection is focused on developing an estimate of the magnitudes of forces in these members. Since the material presented in these subsections was not presented in a previous report, an overview of the development of the expressions is provided in this report. While an understanding of the development of these expressions can help provide designers a better feel for the origin of the equations, simply reviewing the numerical example presented later in the chapter can also provide engineers with a good understanding of the deformational control provided by the external braces.

The goal of the end result of this derivation is to determine the required spacing, L_{max}, between the external K-frames to adequately control the girder twist to some desired tolerance. The desired tolerance will be based upon control of the relative deformation between adjacent

girders that was labeled $\Delta_{REL\ B\text{-}C}$ in Figure 5.1. To develop expressions for this control, an understanding of the vertical and torsional deformations that occur in the box girder is necessary. In general, the external braces provide control of the relative vertical deformation of adjacent girders. Considering the behavior of one girder, the total vertical deformation can be summarized in the following equation:

$$\Delta = \Delta_{bending} + \Delta^{Global}_{Rotation} + \Delta^{Local}_{Rotation} \tag{5.1}$$

The components of the deformation are demonstrated pictorially in Figure 5.3. Figure 5.3a represents the total deformation of the box girder that can be divided into three components. The component $\Delta_{Bending}$ is shown in Figure 5.3b, which represents the vertical girder deflection related to flexural bending of the box girder. This component can be found by treating the curved girder as a straight girder and computing the flexural deformation. While expressions are available for the variation in deflection along the girder length, the maximum value is typically of interest and that occurs at midspan. Treating the girder as simply supported with a uniform distributed load of w, the maximum centerline bending deformation is:

$$\Delta_{Bending\ \max} = \frac{5wL^4}{384EI} \tag{5.2}$$

where, w is the magnitude of the uniformly distributed load (wt./length), L is the span length, E is the modulus of elasticity of the girder material, and I is the moment of inertia about the axis of bending. For continuous girders this is obviously a conservative representation.

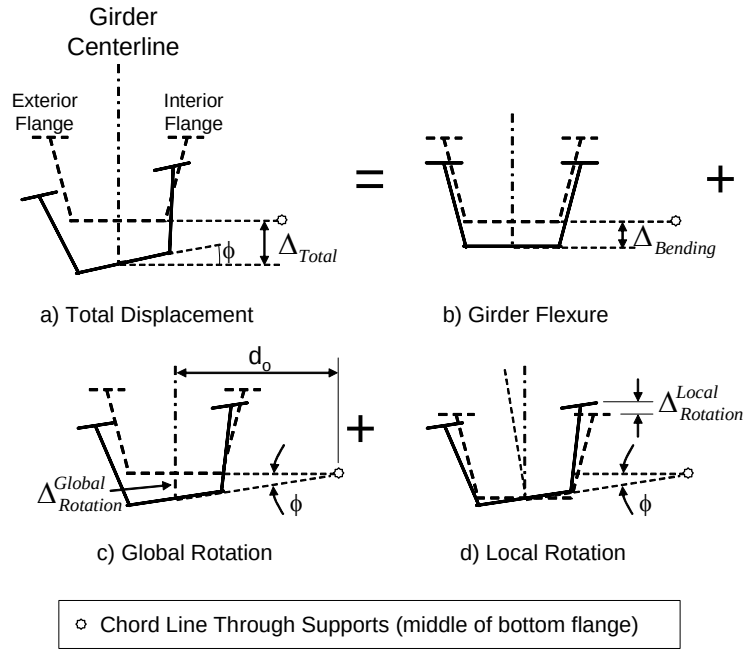

Figure 5.3 Midspan Components of Vertical Box Girder Deformation

The deformation due to twisting of the girders from horizontal curvature has been broken up into a component from "Global Rotation" and a component from "Local Rotation". The

component due to "Global Rotation" depicted in Figure 5.3c represents the vertical deformation that the centerline of the box experiences due to the girder twisting about the chord line of the horizontal curvature of the girders. The chord line of the girders relative to the curved centerline of the box is depicted in Figure 5.4.

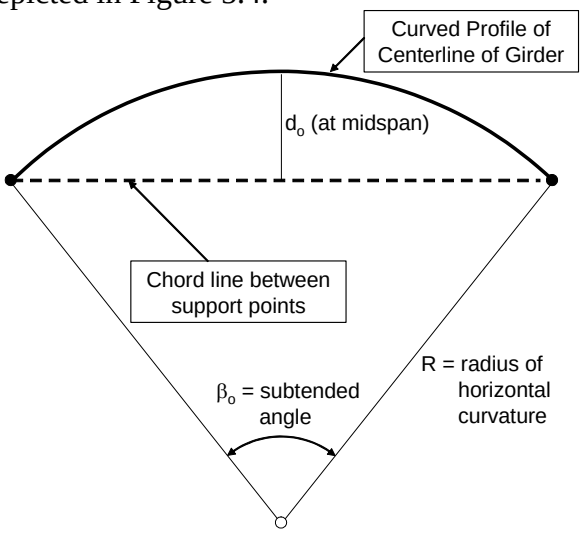

Figure 5.4 Plan View of Girder Centerline Relative to Center of Horizontal Curvature

Based upon the geometry in Figure 5.4, the distance from the girder centerline to the chord line at midspan is given by the following expression:

$$d_o = R\left(1-\cos\left(\frac{\beta_o}{2}\right)\right) \tag{5.3}$$

where, R is the horizontal radius of curvature and β_o is the subtended angle as denoted in the figure. Therefore, at midspan the centerline deformation due to global rotation of the girder would be given by the expression:

$$\Delta_{Rotation}^{Global} \approx \phi(d_o) \tag{5.4}$$

where ϕ is the midspan twist of the girder give by the expression:

$$\phi = \frac{5wL^4}{384EIR}\left(1+\frac{EI}{GJ}\right) \tag{5.5}$$

All of the terms in Equation 5.5 have been defined above except G and J, which are the respective elastic shear modulus and the torsional constant.

The first two components that are discussed above, $\Delta_{Bending}$ and $\Delta_{Rotation}^{Global}$ represent vertical deformations of the centerline of the box girder. The last component, $\Delta_{Rotation}^{Local}$, that is depicted in Figure 5.3d is a local deformation that varies across the width of the girder cross-section.

Since the girder rotates about the shear center, points inside of the shear center along the radius of curvature will "deflect" upwards relative to points outside the radius of curvature due to local twisting of the girder. If the distance from an axis through the shear center to the point "i" that is under consideration is represented as "C_i", the deformation due to this local rotation is given by:

$$\Delta_{Rotation}^{Local} \approx \phi(C_i) \tag{5.6}$$

Figure 5.5 shows the 4 points of primary interest that define the values of the critical slab thickness. Points A and D represent the locations at the edge of the slab where the slab finishing machine (screed) rides on the rails. The slab will be finished to a line that is parallel to the line joining A and D. Points A and D can therefore be taken as the anchor points for a straight line that would represent a uniform slab thickness. The points labeled B and C represent the tips of the top flanges. Because of the local twists of the girders, ϕ_{ext} and ϕ_{int}, the slab thickness will deviate from a uniform thickness by the amounts Δ^*_B and Δ^*_C as denoted in the Figure 5.5b. The distances to the points A, B, C, and D are represented as C_A, C_B, C_C, and C_D, respectively. In most practical cases, C_A=C_D and C_B=C_C and for simplicity, this assumption is applied below.

To predict the errors in slab thickness, the deformed positions of Points A, B, C, and D need to be evaluated using Equation 5.1. If the deck were to have a uniform thickness, points B and C would lie on the straight line drawn between the screed rails in Figure 5.5b. The slope of this line relative to the horizontal is represented by ϕ^* and is given by the following expression:

$$\begin{aligned}
\phi^* &= \frac{\Delta^*_D - \Delta^*_A}{a+b+C_A+C_D} \\
&= \frac{(-\Delta_{w,\text{int}} + \phi_{w,\text{int}} C_D) - (-\Delta_{w,ext} - \phi_{w,ext} C_A)}{a+b+2C_A} \\
&= \frac{(\Delta_{w,ext} - \Delta_{w,\text{int}}) + (\phi_{w,ext} + \phi_{w,\text{int}}) C_A}{a+b+2C_A} \\
\phi^* &\approx \frac{(\Delta_A - \Delta_D)}{a+b+2C_A} = \frac{(\Delta_{bending.ext} - \Delta_{bending.\text{int}}) + (\phi_{ext} - \phi_{\text{int}}) d_o + (\phi_{ext} - \phi_{\text{int}}) C_A}{a+b+2C_A}
\end{aligned} \tag{5.7}$$

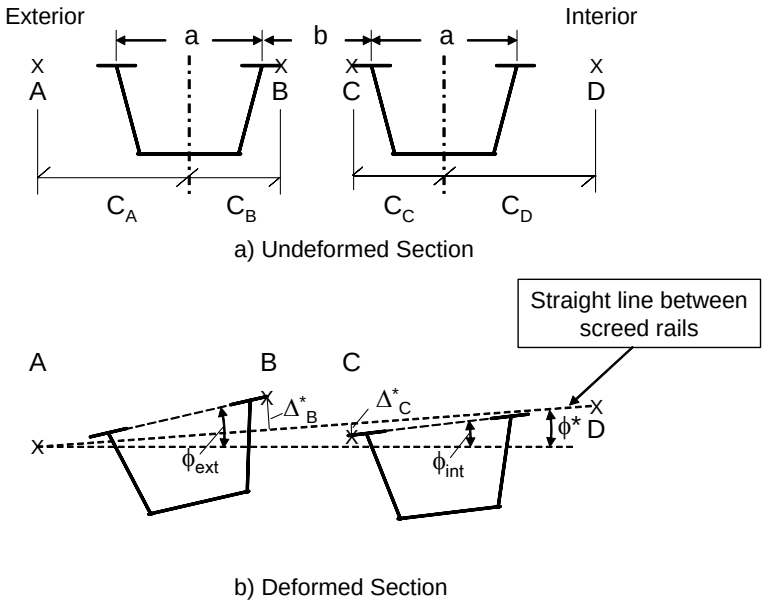

Figure 5.5 Critical Locations Affecting Slab Thickness

Since the screed rails are supported on the overhang brackets, the line joining the top flanges with twists labeled ϕ_{ext} and ϕ_{int} will pass through the respective points labeled A and D. Therefore the expression for $\Delta^*_B = (\phi_{ext} - \phi^*)(C_A + C_B)$ and a similar expression exists for Δ^*_C such that the relative deviation from the uniform slab thickness is given by the expression:

$$\Delta_{\max} = \Delta_{REL\,B-C} = \left|\Delta^*_B\right| + \left\|\Delta^*_C\right\| = (\phi_{ext} + \phi_{int} - 2\phi^*)(C_A + C_B) \qquad (5.8)$$

The goal of this derivation is to determine the maximum spacing between the external diaphragms that will limit the value of Δ_{max} less than some critical value $\Delta_{critical}$, specified by the designer. If the respective spans of the exterior and interior girders are L_e and L_i, the following variables can be defined: $L_{\max} = (L_e + L_i)/2$, and the difference in length between the exterior and interior girders is $\Delta L = (L_e - L_i)/2 = \beta_o(a+b)/2$. Using these definitions and substituting Equations. 5.2-5.7 into Equation 5.8 and simplifying produces the following expression for the maximum change in thickness from a uniform slab thickness, Δ_{max}:

$$\Delta_{\max} = \left(\frac{C_A + C_B}{C_A + \frac{a+b}{2}}\right)\frac{5w\Delta L(L_{\max})}{384EI}\left\{(L_{\max})^2\left[2\left(1+\frac{EI}{GJ}\right) - 8\left(1+\left(1+\frac{EI}{GJ}\right)\left(1-\cos\frac{\beta_o}{2}\right)\right)\right]\right.$$
$$\left. + (\Delta L)^2\left[6\frac{EI}{GJ} - 8\left(1+\left(1+\frac{EI}{GJ}\right)\left(1-\cos\frac{\beta_o}{2}\right)\right)\right]\right\} \qquad (5.9)$$

Further simplifications can be made by recognizing that $(\Delta L)^2 << (L_{max})^2$ and the terms $\left(1+\frac{EI}{GJ}\right)\left(1-\cos\frac{\beta_o}{2}\right)$ can be conservatively neglected. This results in the following expression:

$$\Delta_{max} = \left(\frac{C_A + C_B}{C_A + \frac{a+b}{2}}\right) x \frac{5w(L_{max})^3(\beta_o(a+b))}{384EI}\left[\frac{EI}{GJ} - 3\right] \tag{5.10}$$

For design the maximum permissible deviation in slab thickness (Δ_{max}) can be set equal to some critical value, $\Delta_{critical}$ and the maximum spacing between cross-frames can be solved for, which yields the following expression:

$$L_{max} = \left[\frac{\Delta_{critical}\dfrac{C_A + \frac{a+b}{2}}{C_A + C_B}}{\dfrac{5w\beta_o(a+b)}{384EI}\left(\dfrac{EI}{GJ} - 3\right)}\right]^{1/3} \tag{5.11a}$$

The terms in the numerator next to the $\Delta_{critical}$ are simply dimensions based upon the geometry of the bridge which in most cases is between approximately 1.2 and 1.3. A value of 1.2 will be conservatively assumed. The value of $\Delta_{critical}$ represents the relative displacement between the flanges and was depicted as $\Delta_{REL\ B\text{-}C}$ in Figure 5.1. Although the designer can establish any desired limit for $\Delta_{critical}$, a reasonable limit can be taken as 0.5 in. Applying these assumptions, Equation 5.11a reduces to the following:

$$L_{max} = \left[\frac{0.6}{\dfrac{5w\beta_o(a+b)}{384EI}\left(\dfrac{EI}{GJ} - 3\right)}\right]^{1/3} \tag{5.11b}$$

5.2.3 Forces in Intermediate External K-frames

To develop expressions for the forces in the external diaphragm, the case of a single external K-frame located at midspan will be considered. The lengths, L_i and L_e, of the respective interior and exterior girders in these derivations are taken as the total arclength of the respective girders between the supports. In cases with more than one intermediate cross-frame, it would be conservative to still use the total arclength of the span to determine the design K-frame forces. Another reasonable approach might be to use the total distance

between the braces on either side of the brace in question, which is denoted as L_{eff} in Figure 5.6.

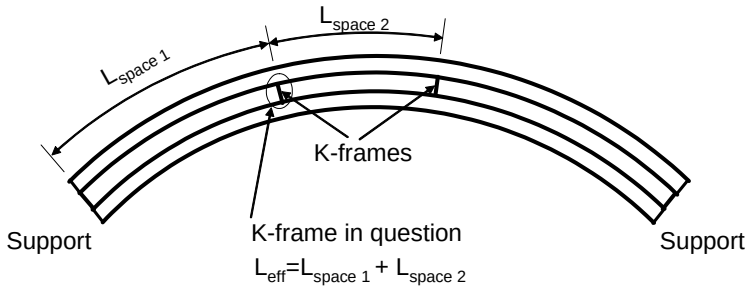

Figure 5.6 Effective Length With More Than One Intermediate Brace

The external diaphragms help to restrain twist and vertical deflections of the box girders at the location of the braces. The basic geometry of the external K-frame and box girder system are shown in Figure 5.7. The width of the boxes between the middle of the top flanges is denoted as "a", while the clear spacing between the girder top flanges is represented by "b". The angle of the diagonal of the K-frame is represented as ψ, while the depth of the K-frame is denoted as h_K. The rotation of the two girders and the K-frame system are assumed to be the same and are represented as ϕ. The distance from the center of a girder to where the top chord of the K-frame connections is shown as L_T. The distances h_K and L_T will be used to represent the torque exerted by the external K-frame on the girders.

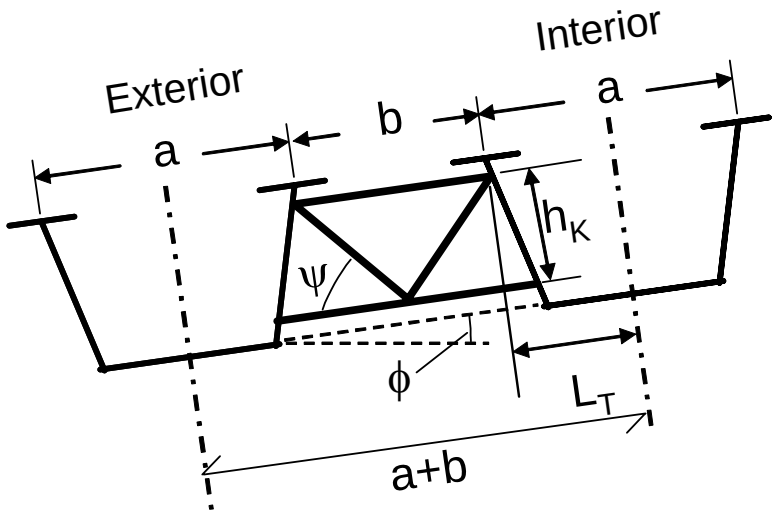

Figure 5.7 Geometry of Girders and K-Frame

The K-frames exert restraining forces H and V on the girders in the respective horizontal and vertical directions. The equal and opposite forces that act on the K-frame are depicted in Figure 5.8a. The corresponding member forces that develop in the K-frames are depicted in Figure 5.8b.

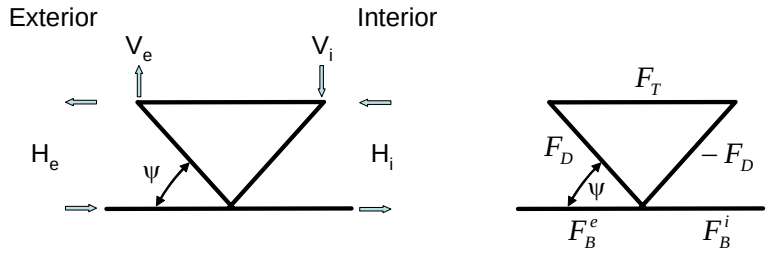

Figure 5.8 Forces on K-Frame

Considering equilibrium of the K-frame in Figure 5.8 leads to the following expressions:

$$H_i = F_D \cos\psi - F_T \tag{5.12}$$

$$H_e = F_D \cos\psi + F_T \tag{5.13}$$

$$V_i = V_e = V = F_D \sin\psi \tag{5.14}$$

The forces from the K-frame on the girders result in a torque T_K and a vertical force V. Based upon the h_K and L_T distances depicted in Figure 5.7 and the reactive forces in Figure 5.8a, the torque from the K-frame on the girder are given by the expression:

$$T_K = Hh_K + VL_T \tag{5.15}$$

The maximum twist occurs at midspan (Appendix A2) and the change in twist caused by the diaphragm is given in the following expression:

$$\Delta\phi_T\left(at\ L/2\right) = \frac{TL}{4GJ} \tag{5.16}$$

The vertical deformation from the vertical shear, V, that comes the shear is given by the following expression (K_o expression given in App. A2):

$$\Delta_V\left(at\ L/2\right) = K_o \frac{VL^3}{48EI} \tag{5.17}$$

where: $$K_o = 1 + \left(1 + \frac{EI}{GJ}\right)\left(1 - \cos\left(\frac{\beta_o}{2}\right)\right) \tag{5.18}$$

and E is the modulus of elasticity, I is the moment of inertia about the axis of bending, G is the shear modulus, J is the torsional constant, and β_o is the subtended angle.

Assuming the axial deformations in diaphragm is very small compared to the girder twist that is restrained, the two girders and diaphragm would all have the same rotation, which is given by the following expression:

$$\phi \approx \tan\phi = \frac{\left(\Delta_w + \Delta_V\right)_{ext} - \left(\Delta_w + \Delta_V\right)_{\text{int}}}{a+b} \tag{5.19}$$

Where Δ_W and Δ_V are the are the respective vertical deformations due to the gravity load, w, and the K-frame shear, V. Equation 5.17 gives the value for Δ_V, while Δ_W would be given by Equation 5.2.

The twist can also be found by simply considering the twist rotation that comes from the applied load (w) minus the change in twist from the diaphragm given in Equation 5.16. This leads to the following expression:

$$\phi = \phi_{w,ext} - \Delta\phi_{ext} = \phi_{w,\text{int}} - \Delta\phi_{\text{int}} \tag{5.20}$$

The equations for the K-frame member forces can then be found by substituting equations 5.12-5.19 into Equation 5.20. This therefore yields the expressions given below.

Summary of member forces:

$$F_D = 4GJ\,\frac{L_i\phi_{w,ext} + L_e\phi_{w,\text{int}} - K_1\Delta_{w,rel}}{K_2} \tag{5.21}$$

$$F_T = \frac{4GJ(\phi_{w,ext} - \phi_{w,\text{int}}) - F_D L_K (L_e - L_i)}{h_K(L_i + L_e)} \tag{5.22}$$

$$F_B = \pm F_D\cos\psi - F_T \tag{5.23}$$

Where,

$$L_K = h_K\cos\psi + L_T\sin\psi$$

$$K_0 = 1 + \left(1 + \frac{EI}{GJ}\right)\left(1 - \cos\frac{\beta_0}{2}\right)$$

$$K_1 = \frac{L_i + L_e}{a+b}$$

$$K_2 = K_0K_1\,\frac{L_i^3 + L_e^3}{12(EI/GJ)}\sin\psi + 2L_iL_eL_K$$

$$\Delta_{w,rel} = K_0\,\frac{5w}{384EI}\left(L_e^4 - L_i^4\right)$$

$$\phi_{w,\text{int}} = \frac{5wL_i^4}{384EIR_{\text{int}}}\left(1 + \frac{EI}{GJ}\right)$$

$$\phi_{w,ext} = \frac{5wL_e^4}{384EIR_{ext}}\left(1 + \frac{EI}{GJ}\right)$$

5.2.4 Design Example of Intermediate External Diaphragm

[Note: A new example is currently being formulated with a longer span (~250 feet) so that an external K-frame is required. The example will appear in the final printing of the document.]

A sample twin box girder section property is given in Figure 5.9. It is a 160 feet single span curved bridge with 600 feet radius of curvature. The width of the bridge deck is 37.5 feet. The box girders are simply supported at the center of the bottom flange for bending at end supports. The twist of the curved girder is restricted at end supports. A 2 kip/ft dead load is applied on each girder.

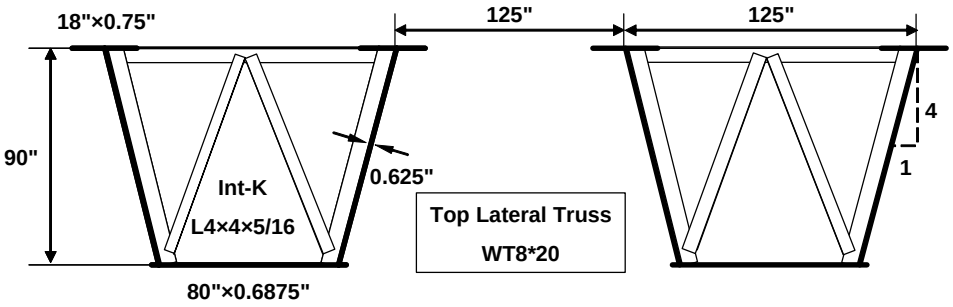

Figure 5.9 Section Property of Curved Box Girder

Using equivalent plate method (Kollbrunner and Basler, 1969), the torsional constant of the quasi-closed section of trapezoidal box girder is computed.

J = 97,000 inch^4 And
I = 234,000 inch^4

$$\beta_0 = \frac{L}{R} = \frac{160}{600} = 0.2667 \quad rad = 15.28°$$

$$\frac{EI}{GJ} = \frac{29000 \times 234000}{112000 \times 97000} = 6.3$$

$$a = b = 10.4'$$

$$L_i = L(\frac{R-b}{R}) = 160 \times (\frac{600-10.4}{600}) = 157.22'$$

$$\Delta_{w,\text{int}}(\frac{L}{2}) = \frac{5wL_i^{\ 4}}{384EI} = \frac{5 \times 2 \times 157.22^4}{384 \times 29000 \times 234000/144} = 0.359' = 4.31"$$

$$\phi_{w,\text{int}}(\frac{L}{2}) = \frac{5wL_t^4}{384EIR_{\text{int}}}(1+\frac{EI}{GJ}) = \frac{5 \times 2 \times 157.22^4}{384 \times 29000 \times 234000/144 \times 589.6}(1+6.3)$$

$$= 0.00417 \quad rad$$

$$d_0 = \frac{R_{\text{int}} + R_{ext}}{2}(1-\cos\frac{\beta_0}{2}) = 600' \times (1-\cos 7.64°) = 64"$$

$$L_e = L(\frac{R+b}{R}) = 160 \times (\frac{600+10.4}{600}) = 610.4'$$

$$\Delta_{w,ext}(\frac{L}{2}) = \frac{5wL_e^{\ 4}}{384EI} = \frac{5\times 2\times 162.78^4}{384\times 29000\times 234000/144} = 0.413' = 4.95''$$

$$\phi_{w,ext}(\frac{L}{2}) = \frac{5wL_e^4}{384EIR_{ext}}(1+\frac{EI}{GJ}) = \frac{5\times 2\times 162.78^4}{384\times 29000\times 234000/144\times 610.4}(1+6.3)$$

$$= 0.00463 \quad rad$$

$$C_B = C_C = \frac{b+b_f}{2} = \frac{9+125}{2} = 67''$$

$$C_A = C_D = \frac{37.5\times 12-125-125}{2} = 100''$$

$$\frac{C_A+\frac{a+b}{2}}{C_A+C_B} = \frac{100+(125+125)/2}{100+67} = 1.35$$

$$l_{\max} \le \sqrt[3]{\frac{\Delta_{critic}\dfrac{C_A+\frac{a+b}{2}}{C_A+C_B}}{\dfrac{5w\beta_0(a+b)}{384EI}(\dfrac{EI}{GJ}-3)}} = \sqrt[3]{\frac{0.5*1.35}{\dfrac{5*2*0.2667*(125+125)}{384*29000*234000/144}(6.3-3)}} = 177'$$

Since maximum unbraced $l_{\max} = 177' > 160'$, which is the span length, the intermediate external diaphragm is not necessary.

To check the proposed force equation, one intermediate external diaphragm is assumed. Here, a diaphragm with 60% depth of the box girder height will be designed and the diaphragm is vertically placed in the middle.

$$h_K = 0.6\times 90'' = 54'' = 4.5'$$

Since the slope of web is ¼, L_T is

$$L_T = \frac{125''}{2} - 0.2\times 90''\times 0.25 = 58'' = 4.83'$$

$$\psi = \arctan\left(\frac{h_K}{\frac{(b+a)}{2}-L_T}\right) = \arctan\left(\frac{54}{125-58}\right) = 38.9°$$

$$L_K = h_K\cos\psi + L_T\sin\psi = 4.5*\cos 38.9° + 4.83*\sin 38.9° = 6.53'$$

$$K_0 = 1+\left(1+\frac{EI}{GJ}\right)\left(1-\cos\frac{\beta_o}{2}\right) = 1+(1+6.3)\left(1-\cos\frac{15.27°}{2}\right) = 1.065$$

$$K_1 = \frac{L_i + L_e}{a+b} = 15.36$$

$$K_2 = K_0 K_1 \frac{L_i^3 + L_e^3}{12(EI/GJ)} \sin\psi + 2L_i L_e L_K$$

$$= 1.065 * 15.36 * \frac{157.2^3 + 162.8^3}{12 * 6.3} \sin 38.9° + 2 * 157.2 * 162.8 * 6.53$$

$$= 1{,}448{,}000$$

$$\Delta_w = K_0 \frac{5w}{384EI}(L_e^4 - L_i^4) = 1.065 * \frac{5 * 2.0}{384 * 29000 * 234000/144}(162.8^4 - 157.2^4) = 0.6"$$

$$\phi_{w,\text{int}} = \frac{5wL_i^4}{384EIR_{\text{int}}}\left(1 + \frac{EI}{GJ}\right) = \frac{5 * 2.0 * 157.2^4 * 7.3}{384 * 29000 * 234000/144 * 589.6} = 0.00418\,rad$$

$$\phi_{w,ext} = \frac{5wL_e^4}{384EIR_{ext}}\left(1 + \frac{EI}{GJ}\right) = 0.00463\,rad$$

Then

$$F_D = 4GJ \frac{L_i\phi_{w,ext} + L_e\phi_{w,\text{int}} - K_1\Delta_w}{K_2}$$

$$= \frac{4 * 11200 * 97000}{144} \times \frac{157.2 * 0.00463 + 162.8 * 0.00418 - 15.36 * 0.6/12}{1448000}$$

$$= 13.3\ kips$$

$$F_T = \frac{4GJ(\phi_{w,ext} - \phi_{w,\text{int}}) - F_D L_K (L_e - L_i)}{h'(L_i + L_e)}$$

$$= \frac{4GJ(0.00463 - 0.00418) - 13.3 * 6.53(162.8 - 157.2)}{4.5(320)}$$

$$= 9.1 kips$$

$$F_B = \pm F_D \cos\psi - F_T = \pm 13.3 * \cos 38.9° - 9.1 = \begin{cases} +1.3 \\ -19.4 \quad kips \end{cases}$$

Choose proper size of angles from LRFD menu with consideration of Euler buckling. The procedure is omitted.

The 3D FEA results with the same model detailed above gives similar results, see Figure 5.10, in which the equation results are bolded.

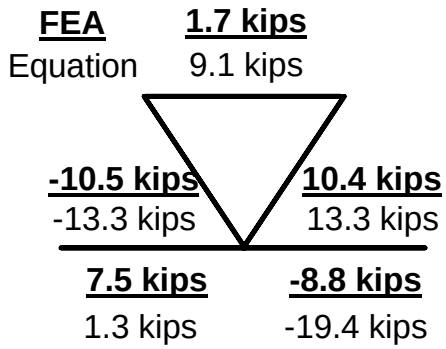

Figure 5.10 Axial Forces of 3D FEA and Equation

5.3 Solid Plate Diaphragms

5.3.1 Introduction

In addition to the external intermediate K-frames, diaphragms are always provided at the ends of the girders. The diaphragms are required for torsional equilibrium of the girder system. Diaphragms resist the girder twist at the ends of the girders based primarily upon the shear stiffness of the diaphragm plates. The ends of the girders are typically closed by solid plates and the diaphragm that connects the adjacent girders is typically trapezoidal in shape. The detailing requirements of the support diaphragms typically depend on the aspect ratio of the end diaphragms. Although the end diaphragm is typically trapezoidal in shape and is often bolted to the two adjacent girders, for establishing the detailing requirements the effective length of the diaphragm can be assumed to be measured as the spacing between the center of the bearings of two adjacent girders as shown in Figure 5.11. For most girder geometries, the practical range of spacing between the bearing centerlines and therefore the effective diaphragm length is in the range of 14 ft. $< L_d <$ 20 ft. Provided the aspect ratio of the diaphragm, $L_d/h_d <$ approximately 5 the diaphragm will generally be governed by the shear stiffness. Considering practical values for L_d range from 14 and 20 feet, the lower range of the diaphragm depth so that shear stiffness dominates the behavior can be established. Shear will dominate the diaphragm stiffness provided the diaphragm h_d is greater than 2.8 feet at the lower L_d range (14 ft.) and 4 feet at the upper L_d range (20 ft.). The end diaphragms are often deeper than these lower bound values, which means that shear stiffness governs the behavior of these braces.

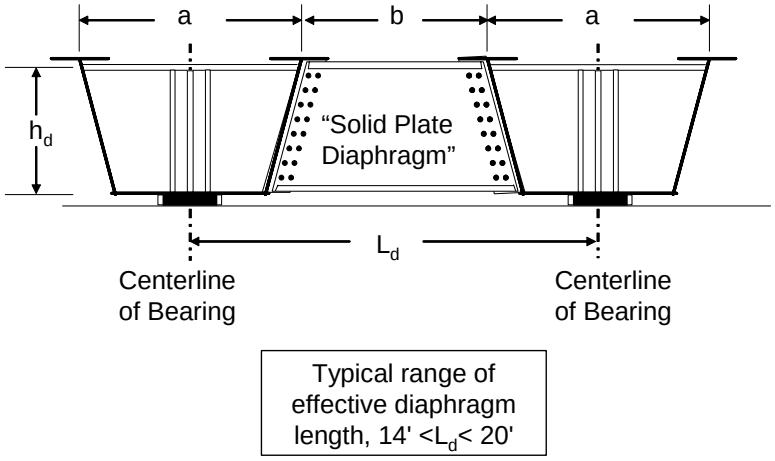

Figure 5.11 Typical End Diaphragm Geometry

The fact that most end diaphragms have aspect ratios less than 5 is important from a detailing perspective. The end diaphragms usually have top and bottom stiffening plates that increase the out of plane stiffness of the diaphragm plates. Many designers associate the top and bottom plates as flanges of a beam and then associate the connection requirements with what is frequently required in the beams of a frame. The flanges of beams in a frame are often fully connected to columns to create a "moment connection" between the beam and column. In the case of the plate diaphragms, the primary mechanism of restraint provided by the diaphragm comes in the shear stiffness of the plates and connecting the flanges has very little effect on the behavior of the system. This is illustrated in Figure 5.12, which shows a three dimensional finite model of the end diaphragm in a twin box girder model.

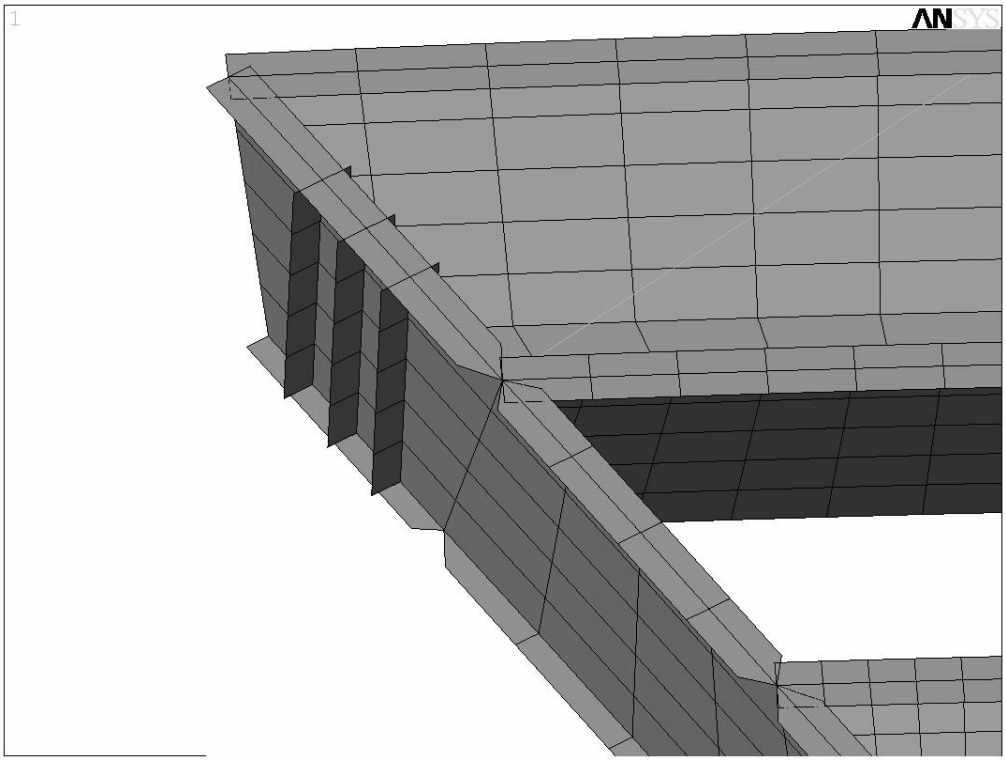

Figure 5.12 Non-Continuous Flanges for Connection Details of plate Diaphragms

The end connections of the solid diaphragm were modeled with both continuous top and bottom plates as well as discontinuous plates as illustrated in Figure 5.12. There was virtually no difference in the behavior of the two girder systems. Only in cases where a relatively shallow diaphragm with an effect aspect ratio in excess of 5 should designers consider making the stiffening plates continuous across the ends of the girders. In most applications, simply bolting the end diaphragm will provide exactly the same behavior as if the top and bottom stiffening plates were connected.

5.3.2 Diaphragm Strength Design Requirements

There are two criteria that the designer should consider when proportioning the solid end diaphragms for box girder applications. The most obvious consideration is the basic shear strength of the plate diaphragm. The other consideration is related to excessive shear deformations at the ends of the beams that can result in rigid body rotations of the girders along the length. The strength limit state is relatively well-understood; however an expression based upon stiffness criteria is also presented in the following sub-section.

Figure 5.13 shows girder torsional demand that acts on diaphragms and the resulting shears that develop as a result of these torsional moments. The moments T1 and T2 are the torsional moments that come as output from the results from a grid model. The girders are generally subjected to vertical gravity loading and although the net end reaction will typically be upwards, the diaphragm tends to redistribute the gravity load so that more of the gravity load shifts towards the exterior girder. Figure 5.13 shows the redistribution in the form of a downward shear on one girder and an upward shear on the other girder. The shear, V,

represents the design shear for the end diaphragm. In terms of the girder end torques, the shear is:

$$V = \frac{T_1 + T_2}{L_d} \tag{5.24}$$

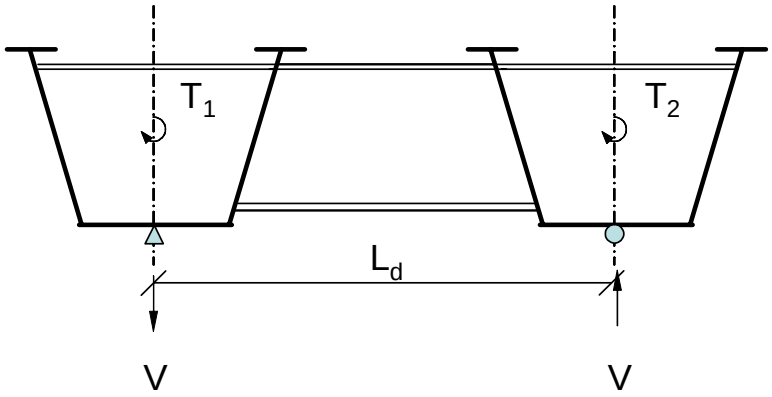

Figure 5.13 Force Demand on External Plate Diaphragm

In a curved girder L_d is the difference in the radii of the two girders. The design approach for shear is based upon a uniform shear stress through the depth of the plate. Referring to the area of the diaphragm plate as $A_d = h_d t_d$, the shear stress would be given as follows:

$$\tau = \frac{V}{A_d} = \frac{T_1 + T_2}{L_d A_d} = \frac{T_1 + T_2}{L_d h_d t_d} \tag{5.25}$$

Based upon a uniformly distributed load on a simply supported girder, the end torque (neglecting the presence of intermediate K-frames) is given by the following expression (Appendix A1):

$$T_i = \frac{wL_i^3}{24R_i} = \frac{wL_i^2\beta_o}{24} \tag{5.26}$$

Where w is the uniformly distributed load, L_i and R_i are the respective chord length and radius of curvature of the ith girder, and β_o is the subtended angle within the span. This leaves the designer with several options to design the plate diaphragm for strength. The torques from Equation 5.26 will also provide reasonable estimates of the design torques. Although the equation was derived for a simply supported girder, there is not much torsional interaction between adjacent spans in box girders since the diaphragms are relatively stiff and the St. Venant stiffness tends to dominate the behavior. Therefore Equation 5.26 provides reasonable estimates of the end torques on each girder. Alternatively, analysis results can also be used such as getting the torques from a grid analysis. With the end torques in the two adjacent girders, the diaphragm shear V can be found using Equation 5.24. Once the diaphragm shear is found it can be compared with shear strength (ie. ϕV_n from the LRFD Specification). For example if the web slenderness satisfies the requirements for full shear yielding, the material shear $\tau = 0.58F_y$ can be applied with Equation 5.25 to give:

$$A_d = \frac{T_1 + T_2}{L_d\left(0.58F_y\right)} \tag{5.27}$$

where F_{yw} is the material yield stress of the web of the diaphragm. For a diaphragm web not satisfying the slenderness limits for full yielding, the appropriate expression for shear buckling can be utilized.

5.3.3 Diaphragm Deformational Limits

Instead of the diaphragm strength limit, an alternative limit on the diaphragm may be shear deformation. The section on the intermediate external K-frames discussed the deformational characteristics of the girders in detail. The role of the intermediate braces was to control the relative vertical movement between adjacent girders. The limit of the relative vertical movement between adjacent girder flanges was labeled $\Delta_{critical}$. A value of $\Delta_{critical}$ = 0.5 in. was selected by the authors as a reasonable limit of the relative vertical deformation that is tolerable between adjacent girders. The relative movement that occurs in the section on intermediate K-frames is due to the torsional flexibility in the girders along the bridge length. Relative vertical deformation between the adjacent girder flanges can also occur due to deformations in the end diaphragms. To develop a deformational limit, some geometrical approximations of the portion of the end diaphragm restraining girder twist must be established. Although the diaphragm itself is usually viewed as a trapezoidal plate, since the plate is fully bolted to the two girders with slip critical bolts, the portion of the diaphragm resisting girder twist will be idealized as a rectangular plate extending form the middle of the two girder bearings as depicted in Figure 5.14 for a total diaphragm effective length of L_d.

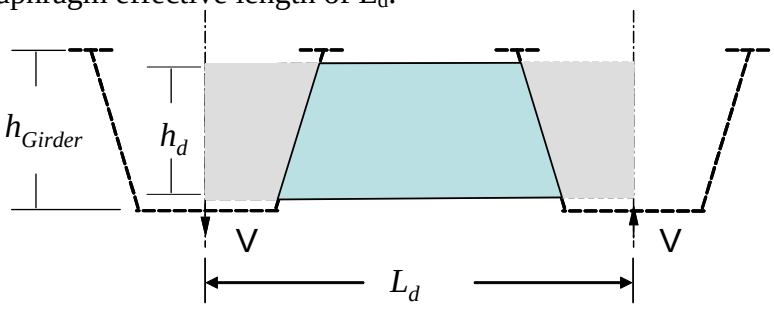

Figure 5.14 Idealized Rectangular Diaphragm Plate

Figure 5.15 shows the girder end deformations at the diaphragm and then the resulting deformations of the idealized rectangular diaphragm plate. As discussed above, the girder deformations result in a rigid body deformation that causes a relative vertical movement between the two flanges of the box girder. The vertical flange deformations are denoted as Δ_f in Figure 5.15. The relative value between the two flanges is then given by the expression:

$$\Delta_{Rel\ dia.} = 2\Delta_f = 2\phi_o x_r \tag{5.28}$$

where ϕ_o is the end twist due to the shear deformations in the end diaphragm, and the distance x_r is denoted in the figure. Since the end diaphragm deformations result in rigid body movements of the entire girder, these deformations are very undesirable and should be kept to a

minimum. As a result the diaphragms should be made relatively stiff to avoid large relative movements between the adjacent girder flanges. The value of tolerable relative movement due to torsional flexibility along the girder length for the intermediate K-frames was denoted as $\Delta_{critical}$ and a value of 0.5 in. was selected by the authors. The limit for rigid body movement due to deformation in the end diaphragm should be substantially less than this. So as to obtain a stiff external diaphragm, the authors imposed a limit of $2\Delta_f < 5\%\ \Delta_{critical} = 0.05(0.5\ in)=0.025$ in. Solving for $\Delta_f = 0.0125$ in. Equation 5.28 can then be rearranged to solve for the limiting value of end twist, ϕ_o:

$$\phi_o \leq \frac{0.0125\,in}{x_r} \tag{5.29}$$

This limit can then be utilized to determine the required diaphragm characteristics to maintain an end twist less than this value. From Hooke's law the relationship between shear stress and shear strain are given by the expression:

$$\gamma_d = \frac{\tau}{G} \tag{5.30}$$

Where τ is the shear stress, G is the shear modulus and γ_d is the shear strain in the diaphragm. The shear strain in the diaphragm plate is shown as a value γ_d in Figure 5.15b. In actuality, from compatibility between the shear diaphragm and the box girder deformation, the shear strain γ_d is equal to the girder end twist ϕ_o, shown in Figure 5.15a. Therefore applying the limit given in Equation 5.29 to the shear strain and combining Equations 5.25 with 5.30 yields the following requirement:

$$\frac{0.0125"}{x_r} \geq \phi_0 = \frac{\Delta_d}{h_d} = \gamma_d = \frac{\tau}{G} = \frac{T_1 + T_2}{GL_d h_d t_d} \tag{5.30}$$

Simplifying this equation, the required web area of external solid diaphragm to satisfy the stiffness criteria is specified in following equation:

$$A_d = h_d t_d \geq \frac{(T_1 + T_2)x_r}{0.0125GL_d} \tag{5.31}$$

The controlling diaphragm area would be the larger value from Equation 5.31 or the strength criteria discussed in the last sub-section.

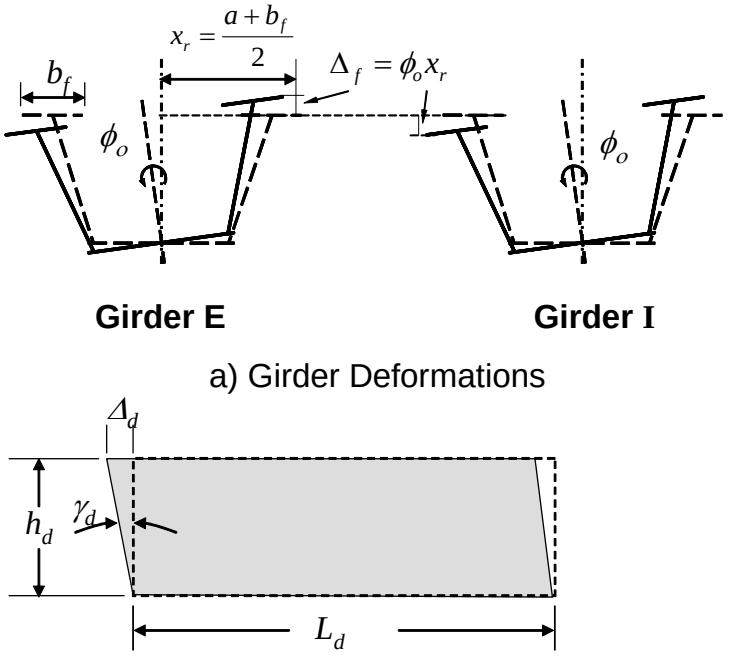

Figure 5.15 Girder and Diaphragm Deformations

Appendix A1

Moment, Torque, Vertical Deflection and Rotation of the Curved Box Girder

A single span girder with radial support is employed in the derivation to show the behavior due to curvature, as shown in Figure A1.

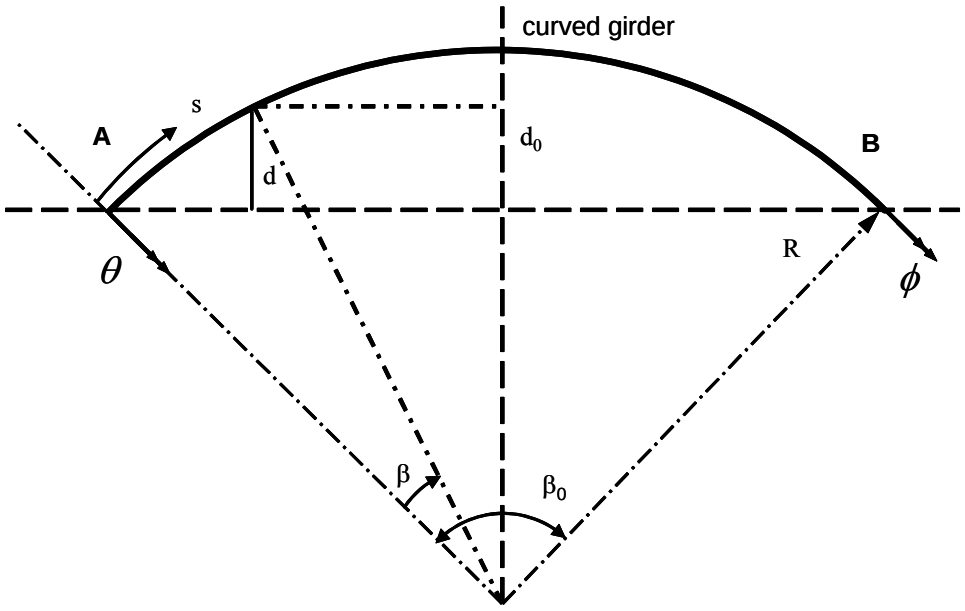

Figure* A1 *Geometry of Curved Girder

For curved girder under self-weight or gravity of concrete deck (distributed vertical load), the girder's deformation has an interaction of bending and twisting.

Tung and Fountain (1970) described the deformation of curved girder with some basic differential equations, shown as Equation A1 ~ Equation A3.

For an infinitesimal segment at subtended angle β, the force equilibrium equation is shown as

$$\frac{dV}{Rd\beta} = \frac{dV}{dx} = -w \tag{A1}$$

$$\frac{dM}{Rd\beta} = \frac{dM}{dx} = -\frac{T}{R} + V \tag{A2}$$

$$\frac{dT}{Rd\beta} = \frac{dT}{dx} = \frac{M}{R} - t \tag{A3}$$

Assumption: T/R term is small and its effect can be neglect for moment.

Then Moment can be approximated as straight girder

$$M = \frac{wx}{2}(L - x) \tag{A4}$$

Torque: for cases only has vertical load w, t = 0

$$\frac{d^3T}{dx^3} = \frac{1}{R}\frac{d(dM/dx)}{dx} = \frac{1}{R}\frac{dV}{dx} = -\frac{w}{R} \tag{A5}$$

Integrating Equation A5 and get the general expression of $T(x)$

$$T(x) = \iiint -\frac{w}{R}dx = -\frac{w}{6R}(x^3 + ax^2 + bx + c) \tag{A6}$$

Boundary conditions:

$$\begin{cases} T(\frac{L}{2}) = 0 \\ T'(0) = T'(L) = 0 \\ T''(\frac{L}{2}) = 0 \end{cases} \tag{A7}$$

Thus, the approximate Torque is

$$T(x) = \frac{wL^2}{24R}(4\frac{x^3}{L^2} - 6\frac{x^2}{L} + L) \tag{A8}$$

Similarly, deformation equilibrium is shown in Equation A9 and Equation A10:

$$\frac{d\phi}{Rd\beta} = \frac{d\phi}{dx} = \frac{\theta}{R} + \frac{T}{GJ} \tag{A9}$$

$$\frac{d\theta}{Rd\beta} = \frac{d\theta}{dx} = \frac{\phi}{R} + \frac{M}{EI} \tag{A10}$$

Where, θ is rotation about the radially (about R-axis) and ϕ is rotation longitudinally. Differentiating Equation A9 by x and substitute Equation A10 and Equation A3, the equation will transform into Equation A11.

$$\begin{aligned} \frac{d^2\phi}{dx^2} &= \frac{1}{R}\frac{d\theta}{dx} + \frac{1}{GJ}\frac{dT}{dx} \\ &= -\frac{\phi}{R^2} + \frac{1}{EI}(\frac{dT}{dx} + t) + \frac{1}{GJ}(\frac{dT}{dx}) \end{aligned} \tag{A11}$$

$\frac{\phi}{R^2}$ usually has small value compared with other terms in the Equation A11. If no distributed torque t is applied, the equation is simplified as Equation A12.

$$\frac{d^2\phi}{dx^2} = (\frac{1}{GJ} + \frac{1}{EI})\frac{dT}{dx} \tag{A12}$$

Thus, the longitudinal rotation of the curved girder is presented as

$$\phi(x) = (\frac{1}{EI} + \frac{1}{GJ})\int_0^x T(s)ds \tag{A13}$$

For curved girder with vertical load w, if substituting the torque Equation A8 into Equation A13, the rotation would be

$$\phi_w(x) = (1 + \frac{GJ}{EI})\int_0^x \frac{T(s)ds}{GJ} = \frac{wL^2}{24R}(\frac{1}{GJ} + \frac{1}{EI})\int_0^x (\frac{4s^3}{L^2} - \frac{6s^2}{L} + L)ds \tag{A14}$$

$$\phi_w(x) = \frac{wx}{24EIR}(1 + \frac{EI}{GJ})(x^3 - 2Lx^2 + L^3) \tag{A15}$$

At mid-span, the maximum rotation is

$$\phi_w(\frac{L}{2}) = \frac{5wL^4}{384EIR}(1 + \frac{EI}{GJ}) \tag{A16}$$

The deflection of curved girder can be approximate by straight girder deflection and curved effect, such as

$$\Delta_w(x) = \frac{wx}{24EI}(x^3 - 2Lx^2 + L^3) + \phi_w(x)d_0 \tag{A17}$$

From Figure A1, $d_0 = R(1 - \cos(\beta_0/2))$, which can be substituted into Equation A17 to give

$$\Delta_w(x) = \frac{wx}{24EI}(x^3 - 2Lx^2 + L^3)[1 + (1 + \frac{EI}{GJ})(1 - \cos\frac{\beta_0}{2})] \tag{A18}$$

$$\Delta_w(\frac{L}{2}) = \frac{5wL^4}{384EI}[1 + (1 + \frac{EI}{GJ})(1 - \cos\frac{\beta_0}{2})] \tag{A19}$$

Appendix A2

Behavior of Curved Girder under Point Torque T

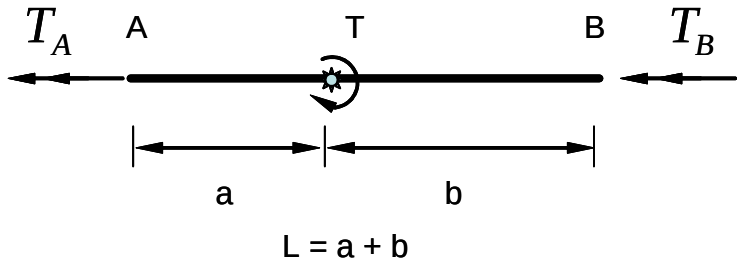

Figure A2 Point Torque on Curved Girder

The torque at the support A and B is approximately in proportion to the distance of loading location to the other support, seen in Equation A20.

$$T_A \approx \frac{b}{L}T = (1-\frac{a}{L})T \tag{A20}$$

$$T_B \approx \frac{a}{L}T = (1-\frac{b}{L})T \tag{A21}$$

$$\phi_T(x) = \frac{1}{GJ}\int_0^x T(s)ds = (1-\frac{a}{L})\frac{Tx}{GJ} \qquad x \le a \tag{A22}$$

$$\phi_T(x) = \frac{1}{GJ}[(1-\frac{a}{L})Ta + \int_a^x T(s)ds] = \frac{Ta}{GJ}(1-\frac{x}{L}) \qquad x > a \tag{A23}$$

If the load is applied at mid-span,

$$\phi_T(x) = \frac{Tx}{2GJ} \tag{A24}$$

$$\phi_T(\frac{L}{2}) = \frac{TL}{4GJ} \tag{A25}$$

Appendix A3

Behavior of Curved Girder under Force V @ Mid-Span

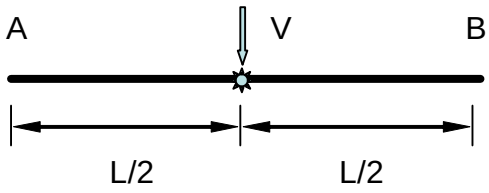

Figure A3 Force on Curved Girder

From LRFD Manual, the maximum deflection for straight girder occurs at the mid-span and the magnitude is

$$\Delta_{V,straight} = \frac{VL^3}{48EI} \tag{A26}$$

And for the curved girder, similar with the case of distributed load,

$$\Delta_V = \frac{VL^3}{48EI}[1 + (1 + \frac{EI}{GJ})(1 - \cos\frac{\beta_0}{2})] \tag{A27}$$

REFERENCES

[AASHTO 2007] AASHTO LRFD Bridge Design Specifications, Fourth Edition, American Association of State Highway and Transportation Officials, 2007.

[Chen et al. 2002] Chen, Brian S., Yura, Joseph A.; and Frank, Karl H., Top Lateral Bracing of Steel U-Shaped Girders, TxDOT Research Report 1395-2F, The University of Texas Center for Transportation Research, Austin, Texas, January 2002.

[Dabrowski 1968] Dabrowski, R. (1968), "Curved Thin-Walled Girders," Cement and Concrete Association, London.

[Fan and Helwig 2002] Fan, Zhanfei; and Helwig, Todd A., "Brace Forces Due to Box Girder Distortion," *ASCE Journal of Structural Engineering*, V. 128, No. 6, pp. 710-718, June 2002.

[Fan 1999] Fan, Z. F., "Field and Computational Studies of Steel Trapezoidal Box Girder Bridges", Ph. D. Dissertation, Civil and Environmental Engineering Department, University of Houston, August 1999.

[Fan and Helwig1999] Fan, Zhanfei; and Helwig, Todd A., "Behavior of Steel Box Girders with Horizontal Top Bracing Systems," *ASCE Journal of Structural Engineering*, V. 125, No. 8, pp. 829-837, August 1999.

[Helwig and Fan 2000] Helwig, T. A., and Fan, Z.F. "Field and Computational Studies of Steel Trapezoidal Box Girder Bridges," TxDOT Research Report 1395-3. The University of Houston, August 2000.

[Helwig et al. 2004] Helwig, T. A., Herman, R., and Li, Dawei "Behavior of Trapezoidal Box Girders with Skewed Supports," TxDOT Research Report 0-4148-1. The University of Houston, May 2004.

[Kim and Yoo 2006] Kim, Kyungsik and Yoo, Chai H., "Brace Forces in Steel Box Girders with Single Diagonal lateral Bracing Systems, ASCE Journal of Structural Engineering, Vol. 132, No. 8, August 2006.

[Kolbrunner and Basler 1969] Kolbrunner, C.F. and K. Basler "Torsion in Structures: An Engineering Approach". Springer-Verlag: Berlin, 1969. pp. 1-21, 47- 50.

[Li 2004] Li, Dawei "Behavior of Trapezoidal Box Girders with Skewed Supports," Ph. D. Dissertation, Civil and Environmental Engineering Department, University of Houston, August 2004.

[Steel Quality Council 2005] Preferred Practices for Steel Bridge Design, Fabrication, and Erection; Texas Steel Quality Council, Texas Department of Transportation, 2005.

[Richardson 1963] Richardson, Gordon, & Associates, Consulting Engineers (1963) "Analysis and Design of Horizontal Curved Steel Bridge Girders", United States Steel Structural Report, ADUSS 88-6003-01.

[Topkaya and Williamson 2003] Topkaya, C. and Williamson, E. B. (2003). "Development of Computational Software for Analysis of Curved Girders under Construction Loads." Computers and Structures, Vol. 81, No. 21, pp. 2087-2098.

[Tung and Fountain 1970] Tung, D. H. and Fountain, R. S., (1970), "Approximate Torsional Analysis of Curved]Box Girders by the M/R Method," Engineering Journal, AISC, Vol. 7, No. 3, pp. 65 - 74.

[TxDOT Bridge Design Manual 2001] TxDOT Bridge Design Manual, Texas Department of Transportation, December 2001.